

Characterization of the Copper Starvation Response in the pMMO-Obligate Methanotrophic Bacterium
Methylomicrobium album strain BG8

by

Phillip Keith Sun

A thesis submitted in partial fulfillment of the requirements for the degree of

Master of Science

in

Microbiology and Biotechnology

Department of Biological Sciences

University of Alberta

© Phillip Sun, 2024

Abstract

Studies on copper as a critical nutrient in methane-oxidizing bacteria (MOB) have mostly focused on the well-characterized “copper switch” in species with dual methane monooxygenase (MMO) variants (Takeguchi & Okura, 2000, Knapp *et al.*, 2007, Kenney *et al.*, 2016). Copper availability dictates which of the two analogous MMO enzymes is used: copper sufficiency favors expression of the copper-associated particulate methane monooxygenase (pMMO) whereas copper depletion favors the iron-associated soluble methane monooxygenase (sMMO) to catalyze the oxidation of methane into methanol (Miyaji *et al.*, 2019, Chang *et al.*, 2021). However, only some MOB, mostly *Alphaproteobacteria* (alpha-MOB), encode sMMO (Takeguchi & Okura, 2000, Fru *et al.*, 2011), while the majority of *Gammaproteobacteria* MOB (gamma-MOB) are pMMO-obligate and lack a “copper switch”; thus, their response to copper starvation has not been as well studied. Under copper deficiency, some MOB produce methanobactin (Mbn), a chalkophore used for scavenging copper from the environment (Fru *et al.*, 2011, Bandow *et al.*, 2012). While Mbn and their respective biosynthetic gene clusters (BGCs) have been well described in alpha-MOB (Semrau *et al.*, 2020), only recently have Mbn been minimally characterized in gamma-MOB (Choi *et al.*, 2010, Kang-Yun *et al.*, 2022). How pMMO-obligate gamma-MOB respond to copper starvation stress represents a gap in our state of knowledge. This study examines the copper starvation response in the gamma-MOB, pMMO-obligate, *Methylobacterium album* strain BG8, which was shown to produce a chalkophore under copper limitation (Kang-Yun *et al.*, 2022). *M. album* BG8 grown under copper deficiency exhibited stunted growth and a smaller cell size; and transcriptomic analysis revealed the shutting down of metabolic activity with selective upregulation of copper acquisition genes. Bioinformatics analysis via a suite of BGC detection and phylogenetic programs reveal a downregulated BGC encoding for siderophore biosynthesis, as well as two intensively upregulated cyanobacterial-related BGCs potentially encoding for a putative Mbn, and a putative ‘toxin’ hereby named methanopeptide (Mpt). Taken together, these results reveal novel natural products involved in alleviating copper starvation stress, underscore the redundant nature of copper acquisition systems in the pMMO-obligate *M. album* BG8, and establish an evolutionary connection in a stress response system between MOB and cyanobacteria.

Dedication

My deepest gratitude to my parents Pamela and Victor and my brother Quin; you are the gentle wind at my back with every step I take, you are the pillars of strength supporting me no matter my state of health, you are the beacons of warmth that continue to light the depths of my labyrinth mind. I profoundly venerate my shepherds Uncle Bill and Aunt Helen; you steered me here to the University you love and governed, made me home away from home, and always encouraged me to chart my own course no matter the squalls. To my friends, lab mates, fellow teaching assistants and colleagues, I am ever thankful for your companionship and tutelage; you are the humble traveler offering a stranger your camp and hearth, the unreserved dancer with the inviting hand outstretched, the kindred spirit giving unto me always your better self however fleetingly long our journeys intertwine. Lastly, I am indebted to my supervisors Dr. Lisa Stein and Dr. Dominic Sauvageau; you guided me with your steady hand, taught me how to learn, and gifted me your enduring compassion throughout my years of absence and inactivity whilst I dwelled on comprehending my own human condition, dreaming upon infinite hypotheticals, and waking to few definitive answers. One infallible truth I have ascertained is that I am blessed to have around me people who are generously loving, kind, and inspiring.

Thank you for being the angels you are, thank you for being you.

Acknowledgements

Many thanks to Dr. Lisa Stein and Dr. Dominic Sauvageau in their capacity as supervisors, and Dr. Jon Dennis as the arms-length committee member.

This research was made possible through assistance provided by the University of Alberta, The Natural Sciences and Engineering Research Council of Canada, Alberta Innovates, and Future Energy Systems.

Table of Contents

Abstract.....	ii
Dedication.....	iii
Acknowledgements.....	iv
List of Figures	vii
List of Common Abbreviations	viii
(1) Introduction.....	1
(2) Literature Review	3
(2.1) The methane cycle and methane oxidizing bacteria	3
(2.2) Methane oxidation regulated by a “copper switch”	5
(2.3) Rare earth elements vs calcium cofactors in methanol oxidation	7
(2.4) Completing carbon oxidation and bioassimilation.....	8
(2.5) Biosynthetic gene clusters and their natural products.....	8
(2.6) Siderophore and methanobactin	9
(2.7) <i>In silico</i> characterization of biosynthetic gene clusters	11
(2.8) Methane-oxidizing bacteria at the crossroads of nutrient cycling.....	14
(2.9) <i>Methylomicrobium album</i> BG8.....	15
(3) Methods	19
(3.1) Media preparation	19
(3.2) Culturing and growth measurements of <i>M. album</i> BG8.....	19
(3.3) RNA extraction and transcriptomic analysis	20
(3.4) Bioinformatic analyses of biosynthetic gene clusters	21
(4) Results	23
(4.1) Copper deficiency stunts growth of <i>M. album</i> BG8	23
(4.2) Transcriptome reveals a uniform, selective, copper starvation response	24
(4.3) Analysis of three differentially expressed biosynthetic gene clusters and their natural products	27
(5) Discussion	32
(5.1) The case for a cyanobactin-like methanobactin.....	32
(5.2) Inferring the function of novel "methanopeptide"	35
(5.3) An ancestral nutrient stress response links methane oxidizing bacteria to cyanobacteria	36
(6) Conclusion.....	39
(7) References	41

Appendix..... 53

List of Figures

Literature Review

- Review Image 1. The methane cycle.** 3
- Review Image 2. Methane oxidation pathway of methane oxidizing bacteria.** 5

Results

- Figure 1. Cell morphology and growth of *M. album* BG8.** 23
- Figure 2. Heatmaps of differentially expressed genes of *M. album* BG8 chromosome and plasmid.** 25
- Figure 3. Heatmaps of significant differentially expressed BGCs.** 28
- Figure 4. Phylogenetic tree of cyclic peptide type ABC transporters from the domain *Bacteria*.** 30

Discussion

- Figure 5. Putative peptide structure of novel methanobactin.** 34

Conclusion

- Figure 6. Summary figure of copper acquisition mechanisms of *M. album* BG8.** 39

Appendix

- Appendix Figure 1. Physical characterization of *M. album* BG8.** 53
- Appendix Figure 2. Change in concentration of gases measured from headspace of *M. album* BG8 cultures.** 54
- Appendix Figure 3. PCA plots of transcriptome dataset.** 55
- Appendix Figure 4. Gene set enrichment of genes in Gene Ontology terms.** 56
- Appendix Figure 5. Volcano plots of differentially expressed genes.** 57
- Appendix Figure 6. cblaster plot homologous gene clusters.** 58, 59
- Appendix Figure 7. BiG-SCAPE generated plot of related BGCs.** 60
- Appendix Figure 8. Precursor peptide candidates from *M. album* BG8 and closely related species.** 61

List of Common Abbreviations

AOA – ammonia oxidizing archaea
AOB – ammonia oxidizing bacteria
AMO – ammonia monooxygenase
AMS – ammonia mineral salts media
alpha-MOB – alphaproteobacterial methane oxidizing bacteria
antiSMASH – antibiotics & Secondary Metabolite Analysis Shell
BGC(s) – biosynthetic gene cluster(s)
BiG-SCAPE – Biosynthetic Gene Similarity Clustering and Prospecting Engine
EMP – Embden-Meyerhof-Parnas pathway
ETC – electron transport chain
FADH – formaldehyde dehydrogenase
FDH – formate dehydrogenase
gamma-MOB – gammaproteobacterial methane oxidizing bacteria
GC – gas chromatography
GECCO – Gene Cluster prediction with Conditional Random Fields
GHG – greenhouse gas
GSEA – gene set enrichment analysis
HMMs – Hidden Markov Models
Mbn – methanobactin
MC – microcystin
MeDH – methanol dehydrogenase
MIBiG – Minimum Information about a Biosynthetic Gene cluster
MOB – methane oxidizing bacteria
Mpt – methanopeptide
MMO – methane monooxygenase
OD – optical density
pMMO – particulate methane monooxygenase
PP – pentose phosphate pathway
sMMO – soluble methane monooxygenase

NMS – nitrate mineral salts media

NP(s) – natural product(s)

NPAAtlas – the Natural Product Atlas

NRP(s) – non-ribosomal peptides

NRPS – non-ribosomal peptide synthetases

REEs – rare earth elements

RiPP(s) – ribosomally synthesized and post-translationally modified peptide(s)

RODEO – Rapid ORF Description & Evaluation Online

SMILES – Simplified Molecular-Input Line-Entry System

TBDT – TonB-dependent transporter proteins

(1) Introduction

Copper is a crucial nutrient required for efficient methane oxidation in methane-oxidizing bacteria (MOB). The effect of copper on metabolism has been well elucidated in alphaproteobacterial MOB (alpha-MOB), as demonstrated through the well-described “copper switch” mechanism dictating gene expression in species possessing dual methane monooxygenase (MMO) variants (Semrau *et al.*, 2013, Gu & Semrau, 2017), as well as in the biosynthesis and properties of copper-binding chalkophores called “methanobactin” (Mbn) in methanotrophic bacteria (Krentz *et al.*, 2010, Fru *et al.*, 2011). Recent studies of Mbn in the supernatant of gammaproteobacterial MOB (gamma-MOB) cultures indicate that gamma-MOB also produce chalkophores to compete for copper in their environment (Choi *et al.*, 2010, Kang-Yun *et al.*, 2022). One of these Mbn-producing MOB is the particulate MMO- (pMMO) obligate methanotroph *Methylomicrobium album* strain BG8. Little is known about the copper starvation response in pMMO-obligate MOB aside from the absence of both a “copper switch” and genes expressing canonical Mbn previously characterized in alpha-MOB. There has yet to be a systemic examination into how *M. album* BG8 – or any pMMO-obligate MOB – would respond to copper starvation given their lack of an alternative iron-utilizing soluble MMO (sMMO), which suggests they would totally rely on copper as the necessary cofactor for methane oxidation. This leads to multiple important questions. Given that secondary metabolites are often involved in the stress response of bacteria, is Mbn the sole biosynthetic response for *M. album* BG8 to compete for copper? If so, what biosynthetic genes are required for and involved in its production given that the Mbn-producing biosynthetic gene cluster (BGC) of alpha-MOB is absent in gamma-MOB? How do varying nitrogen and carbon sources affect this copper starvation response? Is the response lessened when *M. album* BG8 is grown solely on methanol or increased due to co-metabolism of ammonium? What copper-acquisition redundancies does *M. album* BG8 encode to maintain copper sufficiency in a copper depleted environment?

I centered my research thesis on these questions by characterizing the response of *M. album* BG8 — a fast growing, metabolically adaptable, gamma-MOB — to copper starvation when growing with varying combinations of carbon (methane or methanol) and nitrogen (ammonium or nitrate) sources. The first

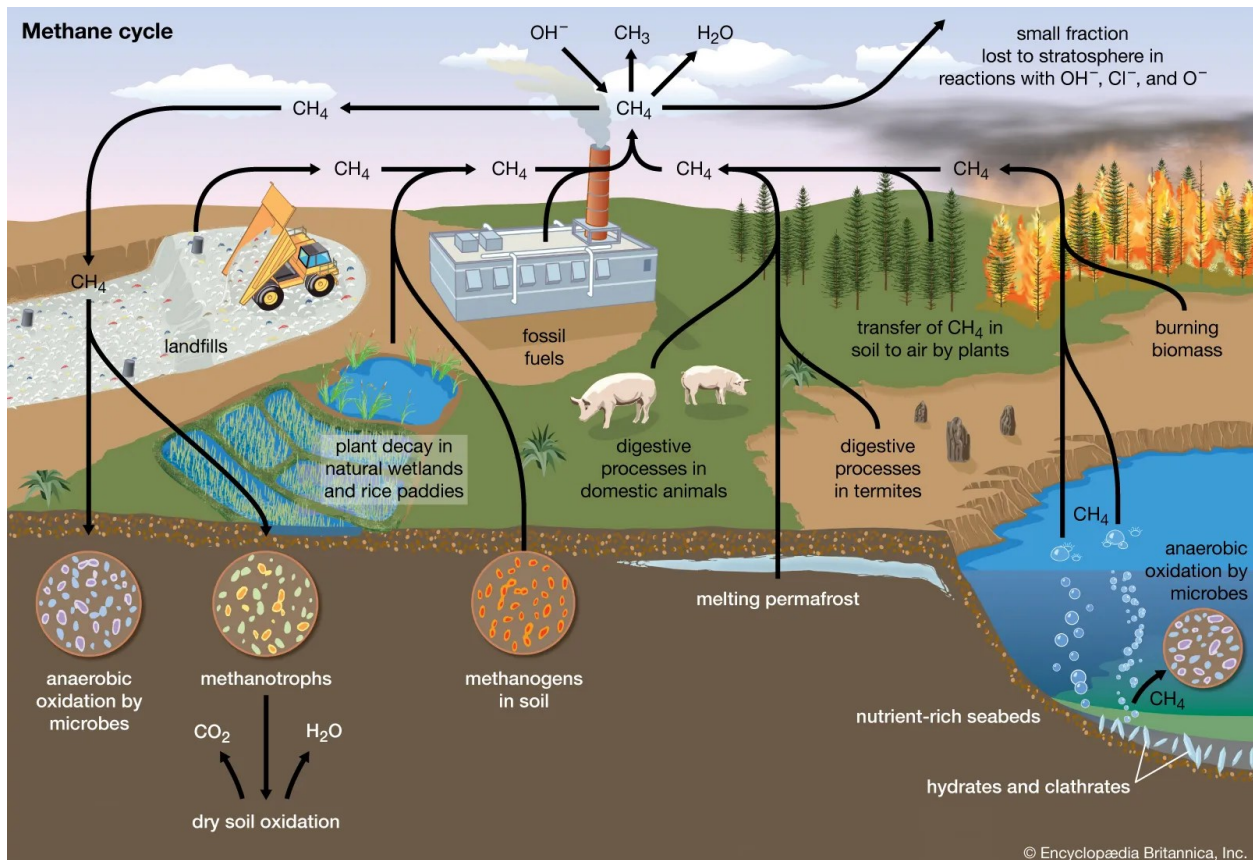
objective was the culturing of *M. album* BG8 in copper-depleted conditions to characterize physically observable traits, such as morphology and growth rate, as indicators of copper starvation stress. The second objective was to extract and sequence mRNA from *M. album* BG8 when grown under 8 combinatorial nutrient conditions with various carbon source (methane or methanol), nitrogen source (nitrate or ammonium), and presence of copper (depleted or replete). Lastly, I analyzed biosynthetic gene clusters (BGCs) statistically validated as differentially expressed in the transcriptome data, along with other genes of significance, to characterize the copper starvation response in its biological context. Elucidating the actors involved in the copper starvation response of *M. album* BG8 contributes to our understanding of gamma-MOB physiology and their response to copper stress. Identification of other differentially expressed BGCs yields further insight into stress response mechanisms of pMMO-obligate gamma-MOB when compared to stress response mechanisms that are better characterized in alpha-MOB that possess both pMMO and sMMO.

The goals outlined by the objectives were achieved through culturing, harvesting, transcriptomic analysis, and bioinformatics analysis of *M. album* BG8. Observations of changes in biomass growth rate, gas consumption/production, and cell morphology were made, and transcriptomic analysis via RNA sequencing was accomplished with mid-log phase cells. A suite of state-of-the-art BGC genome mining/prediction tools revealed copper availability as the most influential factor (over nitrogen and carbon combinations), with highly significant changes in gene expression between copper depleted and replete conditions. Copper starvation shut down general metabolism in *M. album* BG8 and downregulated a siderophore-producing BGC. Conversely, a selection of copper acquisition genes were upregulated, along with two cyanobacterial-related BGCs encoding for a putative Mbn and a novel 'toxin', hereby named methanopeptide (Mpt). This research provides a basic framework for characterizing general stress effects in *M. album* BG8 and similar MOB via *in silico* analyses by employing state-of-the-art BGC prediction software guided by biologically-driven omics-level data.

(2) Literature Review

(2.1) The methane cycle and methane oxidizing bacteria

Methane is a potent greenhouse gas (GHG) with a global warming potential 30 times that of carbon dioxide on a 100-year time scale, and 80 times on a 20-year time scale (IPCC, 2023). A complex web of biotic and abiotic processes governs the fate of methane in natural environments (Review Image 1). 60% of methane emissions are anthropogenic, with agriculture, petroleum, and waste disposal industries as



Review Image 1. The methane cycle. Major methane sources and fates and their abiotic and biotic processes are illustrated (Britannica, 2023. Permissibly reproduced as per publisher's Terms of Service, Section 1).

major emitters. Despite its anthropogenic sources, methane is ubiquitous in nature where it is constantly generated and utilized by microbes, particularly in expanding wetland environments (Niswati *et al.*, 2004, Chowdhury & Dick, 2013, Lee *et al.*, 2014, Cerbin *et al.*, 2022). Decomposition of organic matter in

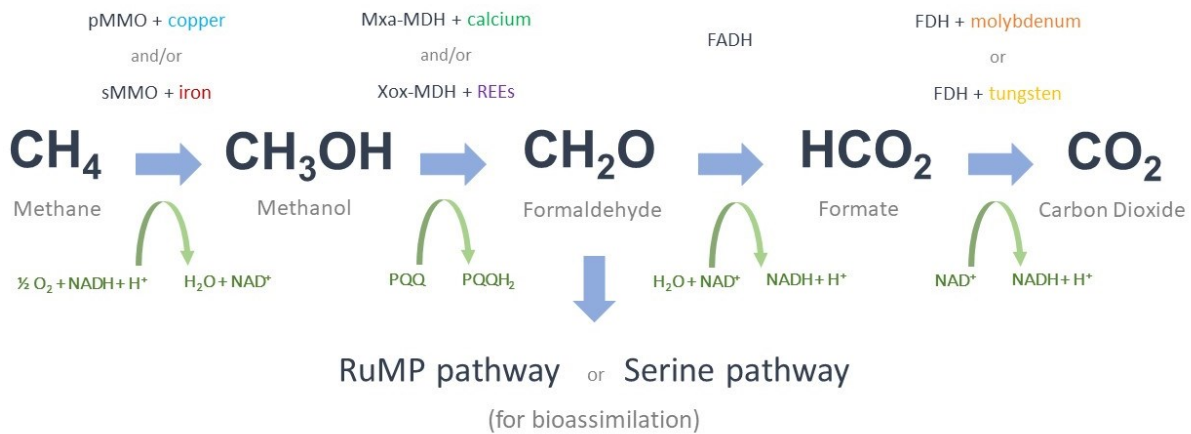
anaerobic environments such as those in soils, lakes, bogs, and oceans via archaea called “methanogens” produces methane as a metabolic waste product. On the other hand, methane is consumed by methanotrophs, or “methane-eating” microbes, that oxidize it as their primary source of energy and carbon (Whittenbury *et al.*, 1970, Hanson & Hanson, 1996, Hakemian & Rosenzweig, 2007). Methanotrophs mitigate the amount of methane emitted to the atmosphere and they serve as the sole biological sink by sequestering methane into biomass and converting it to carbon dioxide. Increasingly frequent wildfires, melting permafrost, and expansion of tropical wetlands brought about by anthropogenically-induced global warming threatens to shift the methane cycle evermore towards a negative feedback loop. Therefore, how the metabolism of methanotrophs is affected by climate change is integral knowledge that we must understand from ecological, biotechnological, and existential perspectives to mitigate planetary warming.

While methane is generated by methanogens in anaerobic environments and potentially oxidized by anaerobic methanotrophs such as bacteria from the candidate phylum NC10 (He *et al.*, 2016) or archaea belonging to *Methanomicrobiales* and *Methanosarcinales* (Knittel & Boetius, 2009), the best-known group of methanotrophs are methane-oxidizing bacteria (MOB) that inhabit mostly aerobic environments. Utilizing oxygen as a preferred terminal electron acceptor, aerobic MOB utilize methane monooxygenases (MMO) to oxidize methane to generate energy and carbon for biomass assimilation (Hakemian & Rosenzweig, 2007). MOB belong to the phylum *Pseudomonadota* (previously *Proteobacteria*) and are further split between two classes consisting of *Alphaproteobacteria* (formerly type II methanotrophs) and *Gammaproteobacteria* (formerly type I methanotrophs) (Hanson & Hanson, 1996). Other lesser known aerobic methanotrophs belong to the phylum *Verrucomicrobia* (Dunfield *et al.*, 2007, Qiu *et al.*, 2009). Within *Alphaproteobacteria*, under the order *Hyphomicrobiales*, are two families of methanotrophs: *Methylocystaceae* and *Beijerinckiaceae*. *Methylocystaceae* contain few genera, but includes *Methylocystis* and *Methylosinus*, in which both the “copper switch” mechanism and Mbn have been extensively characterized (Knapp *et al.*, 2007, Krentz *et al.*, 2010, Fru *et al.*, 2011, Bandow *et al.*, 2012, Farhan Ul Haque *et al.*, 2015, Kenney *et al.*, 2016, Peng *et al.*, 2022). In *Gammaproteobacteria*, MOB are found in the class *Methylococcales* (Orata *et al.*, 2018), and primarily in the family *Methylococcaceae*, that encompasses a greater diversity of genera relative to *Methylocystaceae*. Despite their diversity, aerobic MOB utilize the same methane oxidation pathway with an assortment of enzymes utilizing metals and rare

earth elements as cofactors (Hakemian & Rosenzweig, 2007), with enzyme variants depending on the particular species.

(2.2) Methane oxidation regulated by a “copper switch”

MOB share a common methane oxidation pathway (Review Image 2). While most MOB encode for the copper-containing particulate MMO (pMMO), a minority of gamma-MOB and the majority of alpha-MOB



Review Image 2. Methane oxidation pathway of methane oxidizing bacteria. Enzymes and cofactors involved are shown above the pathway, and co-substrates/products below.

also encode for the soluble variant (sMMO) which uses iron in its active site (Semrau *et al.*, 2018). The expression of the analogous forms of MMO are controlled by a mechanism called the “copper switch”: an abundance of copper results in pMMO expression, whilst in the absence of copper, a switch in gene regulation occurs to repress pMMO expression and upregulate sMMO expression (Semrau *et al.*, 2013, Kenney *et al.*, 2016, Gu & Semrau, 2017).

pMMO has a high affinity for methane, is membrane bound, and utilizes copper to form an intermediate complex with oxygen to oxidize methane into methanol (Lee *et al.*, 2006). It is encoded by the *pmo* operon for 3 subunits: PmoA, PmoB and PmoC (Balasubramanian *et al.*, 2010, Larsen & Karlsen, 2016). Biochemical characterization of pMMO was hindered by difficulty in its heterologous expression due

to its membrane-bound nature and several potential active sites identified for methane oxidation. However, recent cryogenic electron microscopy has clarified the structure and active site of the functional trimer in *Methylococcus capsulatus* Bath, confirming one active site with three copper ions clustered in the PmoB subunit as the site of methane oxidation (Chang *et al.*, 2021). Aside from oxygen and methane as substrates, methane oxidation also requires reducing equivalents in the form of NADH-ubiquinol and protons (Hakemian & Rosenzweig, 2007). Other substrates that can be co-metabolized with pMMO include ammonia, as pMMO is homologous to the ammonia monooxygenase (AMO) utilized by ammonia oxidizing bacteria (Lawton *et al.*, 2014), and a number of short-chain hydrocarbons (Kits *et al.*, 2015). Expression of pMMO is constitutive unless it is actively repressed (for instance in the absence of copper), as it is the dominant version of MMO found in all MOB with a few exceptions of sMMO-only MOB in the *Methylocella* genus (Vorobev *et al.*, 2011). A homolog to pMMO called pXMO can be found in some gamma-MOB; while its function is not well characterized (Tavormina *et al.*, 2011), there is indication that this variant may be preferentially utilized under hypoxic conditions (Kits *et al.*, 2015).

Unlike pMMO, sMMO has been heterologously expressed in *E. coli* and has been better characterized overall than pMMO (West *et al.*, 1992). sMMO has a higher specific rate of catalysis than pMMO, but has relatively poorer affinity for methane, limiting its use under low methane concentrations (Lee *et al.*, 2006). Unlike pMMO which utilizes copper, sMMO has iron as its active-site cofactor. sMMO is encoded by the *mmoXYBZDC* operon and is expressed in the absence of copper. Regulation of the copper switch centers on the protein MmoD, a copper-sensing protein proposed as a transcriptional activator for the *mmo* operon and a transcriptional repressor for *pmo*, as the inverse of this copper switch was observed if *mmoD* gene was knocked out (Semrau *et al.*, 2013). The copper switch is also regulated by the presence of the chalkophore methanobactin (Mbn), amplifying the magnitude of *mmo* activation. Together, this information suggests that both sMMO and Mbn share the same copper switch mechanism and are responsive to low levels of copper; however, the roles of other regulator proteins remain unclear (Knapp *et al.*, 2007, Fru *et al.*, 2011, Semrau *et al.*, 2013, Kalidass *et al.*, 2015).

(2.3) Rare earth elements vs calcium cofactors in methanol oxidation

The next step of the methane oxidation pathway after MMO is methanol oxidation to formaldehyde (Review Image 2), where two forms of methanol dehydrogenases (MeDH) are regulated by a “lanthanide switch” (Akberdin *et al.*, 2018). The canonical MeDH is MxaF, which utilizes calcium as a co-factor and is expressed constitutively in the absence of lanthanide-series rare earth elements (REEs) such as lanthanum, cerium, and samarium. However, when lanthanides are present, an analogous MeDH called XoxF is dominantly expressed and MxaF is repressed (Chu & Lidstrom, 2016, Akberdin *et al.*, 2018, Deng *et al.*, 2018, Zheng *et al.*, 2018, Ito *et al.*, 2021). XoxF-MeDH activity increased 5-10 fold in *Methylobacterium radiotolerans* and *Methylobacterium extorquens* AM1 when grown with lanthanum (Hibi *et al.*, 2011, Nakagawa *et al.*, 2012), as the use of REEs makes methane oxidation more efficient as they are stronger Lewis acids as compared to calcium. However not all REEs are equal; the specific REE in use is also a variable to consider, as “light” REEs such as lanthanum, cerium, praseodymium, and neodymium stimulate more growth in *Methylacidiphilum fumariolicum* SoIV compared to samarium, europium and gadolinium (Pol *et al.*, 2014). The “copper switch” and the “lanthanide switch” are largely independent of each other, although the absence of copper can result in an increased expression of XoxF isoforms (Chu & Lidstrom, 2016, Gu & Semrau, 2017). While XoxF oxidizes methanol to formaldehyde, XoxF-MeDH can also further oxidize formaldehyde directly into formate (Akberdin *et al.*, 2018), bypassing the ribulose monophosphate (RuMP) and serine pathways for carbon assimilation. The acquisition of REEs remain somewhat uncharacterized; several mechanisms for intaking REEs have been proposed, ranging from phosphate transporters previously shown to also uptake metal-phosphates, to chelators such as siderophores/chalkophores with binding affinity to REEs. However, a recent study has determined a TonB-dependent receptor is necessary for the “lanthanide switch” in *Methylovium buriatense* 5GB1C, implying TonB – ExbB – ExbD complexes are involved in the import of lanthanides in MOB (Groom *et al.*, 2019). A protein with high binding affinity to lanthanides named lanmodulin was recently discovered in the methylotroph *Methylorubum extorquens* AM1 (Daumann, 2021).

(2.4) Completing carbon oxidation and bioassimilation

Once oxidized to formaldehyde (Review Image 2), carbon is either assimilated directly through the RuMP pathway, converted to methylene tetrahydrofolate and into the serine pathway (Hanson & Hanson, 1996, Villada *et al.*, 2022), or oxidized to formate via molybdenum-containing or tungsten-containing formate dehydrogenases (FDH) before being ultimately converted to carbon dioxide to regenerate reducing equivalents (Maia *et al.*, 2015). Molybdenum-utilizing FDHs are more common in prokaryotic MOB, whereas tungsten-utilizing FDH are found in methanotrophs living in extreme conditions. Carbon can also be assimilated by a few MOB via the Calvin-Benson-Bassham cycle (Sharp *et al.*, 2014). While some MOB have a complete Calvin cycle for carbon dioxide fixation, the presence of incomplete Calvin cycles in various MOB is perplexing. A recent study on *Methylococcus capsulatus* Bath found the widespread carbon fixation enzyme RubisCo to be essential, indicating that MOB with an incomplete Calvin cycle can still use it for carbon assimilation (Henard *et al.*, 2021).

(2.5) Biosynthetic gene clusters and their natural products

The stress response of bacteria generally includes the production of secondary metabolites to alleviate stress. Many secondary metabolites are produced from the expression of biosynthetic gene clusters (BGCs) and are also commonly referred to as natural products (NPs), with the differing terminology arising from the differing biotechnological/pharmaceutical and physiological/ecological perspectives on their bioactive functions. For example, secondary metabolites with antimicrobial activity produced from BGCs are well researched as NPs used to cure disease, yet their ecological functions may not be as well characterized. Ultimately, they are complex biochemicals produced via diverse suites of enzymes by which they are classified. Classifications include non-ribosomal peptides (NRPs) produced from non-ribosomal peptide synthetases (NRPS) (Nikolouli & Mossialos, 2012) and ribosomally-synthesized and post-translationally modified peptides (RiPPs) (Cao *et al.*, 2021). NRPS are modular enzymes with each module catalyzing a specific step in the synthesis of an NRP. RiPPs are made from ribosomes translating an mRNA

that encodes for a small peptide precursor that is then processed by a protease cleaving off the leader segment from the core peptide with final chemical alterations catalyzed by tailoring enzymes. Unlike proteins, the function of BGC products have been difficult to determine from genomic/protein sequence alone, as NPs can have a wide range of bioactive functions within the same BGC classification (Cheung-Lee & Link, 2019, Navarro-Munoz *et al.*, 2020, Russell & Truman, 2020), notwithstanding the biases in characterizing NPs primarily from a pharmacological perspective (Pishchany & Kolter, 2020). NRPS-derived NRPs from cyanobacteria called cyanopeptides are a good example of this challenge. A great diversity of cyanopeptides produced from a vast suite of modification enzymes have been catalogued and characterized thus far (Welker & von Dohren, 2006, Jones *et al.*, 2021). However, many of these characterizations are minimal, and most research on cyanopeptides has focused on a few toxins such as microcystins, an inhibitor of protein phosphatases that act as a neurotoxin in the liver (Bischoff, 2001, Janssen, 2019). Thus, while cyanopeptides are generally classified as ‘enzyme inhibitors’, their function in an ecological context remains unclear (Egli *et al.*, 2020). An immediate hypothesis for the function of cyanopeptides is one of deterrence against grazing, albeit their widespread presence in all lineages of cyanobacteria suggest their origins predate the emergence of potential grazers (Natumi & Janssen, 2020). Nevertheless, the ecological context regarding the production of microcystins and cyanopeptides during cyanobacterial blooms remains widely debated and is thought to be involved in nutrient and stress adaptation (Natumi & Janssen, 2020). Despite these complications, NPs that have overlapping roles in health and ecology are better characterized in both contexts. One such example of a well characterized NP are siderophores.

(2.6) Siderophore and methanobactin

Siderophores are iron-chelating secondary metabolites (Saha *et al.*, 2013). They are synthesized and mobilized to the extracellular environment to scavenge for iron, an element that is commonly used in biological redox catalysis, yet if not well managed can cause cell damage due to the formation of hydrogen peroxide from the reaction between ferrous iron and water. In infections, pathogens and hosts compete for

iron; pathogenic bacteria often release siderophores in mammalian hosts to acquire iron for rapid growth thus enabling their own pathogenicity, and hosts engage in denying iron by sequestering them away from bacterial invaders (Behnsen & Raffatellu, 2016, Diaz-Perez *et al.*, 2023). In a non-pathogenic context, bacteria employ siderophores to compete with other microbes for iron as well (Behnsen & Raffatellu, 2016). Many siderophores are produced by NRPS. NRPS do not produce a product based on reading mRNA codons and they make only one specific product. Modules of NRPS build a chain of amino acids – of many may be non-proteinogenic – and may also employ polyketide modules. Often circular or branched, these NRPS-derived peptides have a diverse range of additional uses as antibiotics, immunosuppressants, toxins, and more (Feltnagle *et al.*, 2008). Siderophore-producing BGCs have been predicted in MOB, but they have not been well characterized.

Methanobactin (Mbn) are copper-binding siderophores produced by MOB. Although functionally analogous to siderophores, Mbn are not NPs synthesized via NRPS but rather are categorized as RiPPs (Krentz *et al.*, 2010, Kenney & Rosenzweig, 2013). RiPPs are a type of BGC that, unlike NRPs, relies on the ribosome to produce the backbone of the secondary metabolite akin to regular translation, with tailoring enzymes introducing modifications into the mature peptide. Classification of RiPPs is dependent on the structure of the NP: lassomycin – a potent antimicrobial against *Mycobacterium tuberculosis* – is a lassopeptide, consisting of a core peptide cyclized to form a loop with a tail like a 'lasso', with the tail inserted into the loop itself (Gavrish *et al.*, 2014). Classifications can also be based on their origin: cyclic RiPPs produced by cyanobacteria are called cyanobactins and typically possess azol(in)es heterocycles introduced into their peptide structure via tailoring enzymes (Sivonen *et al.*, 2010). The amino acid sequence of a RiPP is encoded via a small ORF that is not typically annotated via regular annotation pipelines. This amino acid sequence is called a precursor peptide and contains a core segment that is modified by various enzymes called tailoring enzymes encoded by the BGC in addition to a leader segment that is cleaved off from the core, leaving the altered core peptide as the mature product (Duan *et al.*, 2022, Rodriguez, 2022). In the Mbn BGC, the precursor peptide MbnA is subsequently modified by tailoring enzymes. Mbn from *Methylocystaceae* are categorized into two distinct groups, both of which belong to the linear azol(in)e-containing peptides binding to copper (I). As suggested by their name, these peptides containazole/azoline rings in their structures and are 'linear' as they do not cyclize as part of modifying the

core peptide like in many other RiPPs (Krentz *et al.*, 2010, Semrau *et al.*, 2020). The biosynthesis of Mbn occurs via a set of core biosynthetic genes: a MbnB-MbnC enzyme cassette binds to the precursor to catalyze and introduce oxazolone rings into the core peptide (Dou *et al.*, 2022), and a MbnF protein is putatively involved in the formation of imidazolone rings. MbnN and MbnS are aminotransferase- and sulfotransferase-tailoring enzymes. MbnT, a TonB-dependent transporter (TDBT), is necessary for methanobactin intake into the cell (Gu *et al.*, 2016). Mbn is the primary mechanism by which competitive interactions occur in the environment for the acquisition of copper. Some MOB compete with other bacteria for copper by producing Mbn with strong binding affinity towards copper, and others compete by intaking foreign Mbn as a form of “theft” (Kang-Yun *et al.*, 2022). Competition for copper can also occur against other microbes such as ammonia-oxidizing bacteria (AOB) and archaea (AOA) that rely on copper as a cofactor in ammonia monooxygenase (AMO); denitrifying bacteria that rely on copper for nitrous oxide reductase; and various other microbes with necessary copper-containing enzymes (Amin *et al.*, 2013, Qin *et al.*, 2018, Zorz *et al.*, 2018). Mbn synthesized by MOB has been demonstrated to sequester and deny copper from denitrifying bacteria, resulting in an increase in nitrous oxide emissions from soils (Chang *et al.*, 2018).

(2.7) *In silico* characterization of biosynthetic gene clusters

Several bioinformatics programs have been created to mine putative BGCs from genomes with varying limitations and usefulness (Kenney & Rosenzweig, 2013). Aside from sequence similarity, these prediction programs rely on the co-occurrence hypothesis that prepose genes involved in biosynthesis of NPs co-occur within BGCs and can therefore be used to search for similar BGCs across genomes. These co-occurring genes are known as core biosynthetic genes: enzymes that are common to the synthesis of closely related natural products. For example, MbnB and MbnC are core biosynthetic genes present in all Mbn-producing BGCs in alpha-MOB. The antibiotics & Secondary Metabolite Analysis Shell (antiSMASH) is the canonical BGC detection and prediction software (Blin *et al.*, 2021), which utilizes a collection of tools to identify gene clusters, determine the presence of enzymes known to be a part of NP-producing

machinery, and categorizing them by product type. This prediction tool can also make rapid comparisons to an internal database of preprocessed BGCs as predicted from genomes, as well as BGCs from the MIBiG repository (Terlouw *et al.*, 2023) that contains minimal information on each BGC that has been experimentally validated. However, while antiSMASH produces predictions on BGC location and function, it is a “rules-based” algorithm dependent on existing research and is limited in detecting or determining the function of novel BGCs. Newer genome mining tools such as DeepBGC (Hannigan *et al.*, 2019), a tool using a deep learning model, uses AI algorithms to search for patterns associated with BGCs and can return predictions on novel BGC candidates, albeit false positives can be high and manual curation is required to determine which predictions are worth pursuing. GECCO is one of the latest iteration of these pattern recognition programs that utilizes conditional random fields and is available and cited despite a lack of intensive peer review (Carroll *et al.*, 2021). A pipeline named ‘funcscan’ incorporates all three BGC detection programs is available via the nf-core framework for community-curated bioinformatics pipelines (Ewels *et al.*, 2020).

While prediction software based on co-occurrence is useful in detecting and categorizing BGCs, it is insufficient for determining the putative function of novel NPs as sequence similarity is not a good predictor of NP function. Therefore, phylogenetic methods are used to supplement information gained based on methods based on co-occurrence. Phylogenetic BGC prediction software relies on the hypothesis that enzymes involved in producing NPs originate via duplication from central metabolic pathways or from other biosynthetic gene clusters. EvoMining was the first program utilizing a phylogenetic approach to infer function by comparing homologs of novel BGCs to curated BGCs (Cruz-Morales *et al.*, 2016, Selem-Mojica *et al.*, 2019). Since then, the latest BGC prediction programs utilize both enzyme recruitment and co-occurrence hypotheses in their algorithms. The Biosynthetic Gene Similarity Clustering and Prospecting Engine (BiG-SCAPE) (Navarro-Munoz *et al.*, 2020) takes outputs from antiSMASH to align functional regions of BGCs using Pfam Hidden Markov Models (HMMs) for subsequent network and phylogenetic analysis. Detection of RiPP BGCs is particularly difficult as there are fewer of them characterized as compared to other secondary metabolites (Terlouw *et al.*, 2023). RiPPER is a program for detecting novel RiPPs (Santos-Aberturas *et al.*, 2019) by utilizing a “bait” tailoring enzyme identified to be involved in RiPP maturation via the Rapid ORF Description & Evaluation Online (RODEO) tool (Tietz *et al.*, 2017). It takes

the “bait” enzyme to identify homologs in hundreds of genomes, then it matches co-occurring genes between the query BGC and the genomic neighborhood of the “bait” homolog, to identify closely related BGCs. Subsequent phylogenetic trees can then be generated to reveal the evolutionary history between the query BGC against curated BGCs containing “bait” homologs. However, unlike proteins, precursor peptides cannot be used as “bait” for homology searches. For example, precursor peptides such as MbNA from Mbn BGCs are small, contain limited conserved regions, and are often not annotated by common annotation pipelines, thus limiting their usefulness for determining the presence of homologous RiPPs.

Despite advances in BGC analysis software, their outputs are only predictions. Thus, supplementation of biologically-driven data is necessary to validate bona fide BGCs. Multi-omics approaches have been suggested as a rapid and systematic means to guide interpretation of the outputs of BGC detection software (Kloosterman *et al.*, 2021). This typically involves coupling transcriptomic and metabolomic data to inform their presence within the genome, and programs integrating these multi-level data sets (Palazzotto & Weber, 2018). Transcriptomic data can be used to inform the presence of BGCs through differential gene expression analysis to identify BGCs within the genome, and several novel BGCs combining these approaches have already been identified (Acharya *et al.*, 2019, Beck *et al.*, 2021). Integrating metabolomics data is more complicated and requires a database of peptide fragments and their corresponding spectra. Tools such as DEREPLICATOR (Mohimani *et al.*, 2017) and the DeepRiPP CLAMS module can be utilized to match isolate spectral peaks corresponding to known modified structures found in NPs and linking them to known modification enzymes and synthases in the genome responsible for these modifications (Merwin *et al.*, 2020). One limitation to these automated programs is recognizing novel modifications and their associated MS/MS spectra, thus *in silico* identification of novel BGCs remains a challenge in active development through programs such as VarQuest, a tool for predicting peptide variants utilizing data on known modifications, and MetaMiner, a tool combining genomics and metabolomics to predict novel modifications (Gurevich *et al.*, 2018, Cao *et al.*, 2019). Another limitation is in obtaining relevant omics data containing their gene expression or NP in the first place. Silent BGCs can be difficult to express if the biological context for their purpose is unknown. Other factors must also be considered

when selecting a suitable omics level for data analysis, as was the case with the low production of *M. album* BG8 Mbn hampering attempts at structural characterization (Choi *et al.*, 2010, Kang-Yun *et al.*, 2022).

(2.8) Methane-oxidizing bacteria at the crossroads of nutrient cycling

Aerobic MOB require methane and oxygen for growth, even though methane production via methanogens occurs in the absence of oxygen. Due to these nutrient requirements, MOB thrive best at the interface between anoxic and oxic conditions (Steinle *et al.*, 2017, Su *et al.*, 2022). However, their role in carbon cycling extends beyond methane as some MOB can fix carbon dioxide via the RubisCo/CBB pathway, and strains such as *Methylovirgula thiovorans* HY1 can fix carbon dioxide at the expense of oxidizing reduced sulfur compounds (Gwak *et al.*, 2022). Furthermore, gamma-MOB have been shown to produce organic products in anoxic ecosystems that can cross-feed other microorganisms, thus acting as primary producers (Kalyuzhnaya *et al.*, 2013, Yu & Chistoserdova, 2017). Combined with the ability of some MOB to oxidize ammonia (Nyerges & Stein, 2009), fix nitrogen (Khadem *et al.*, 2010), and use nitrate/nitrite as terminal electron acceptors (Kits *et al.*, 2015), MOB have a considerable influence on the nitrogen cycle. MOB influence other players in the nitrogen cycle as well; keen competition for copper by MOB results in denying this cofactor to denitrifying and nitrifying bacteria for enzyme biosynthesis (Amin *et al.*, 2013, Zorz *et al.*, 2018, Gorman-Lewis *et al.*, 2019). An enzyme of particular concern is nitrous oxide reductase (NosZ), which enables the conversion of the highly-potent greenhouse gas nitrous oxide to dinitrogen. Mbn has been demonstrated to deny copper to denitrifiers leading to increased production of nitrous oxide in soils (Chang *et al.*, 2018). Similar observations were noted in rice paddies spiked with Mbn and also in microbial consortia dominated by *Methylocystaceae* (Chang *et al.*, 2021).

In summary, MOB thrive at the interface between oxic and anoxic zones/strata, utilize a repertoire of metal-utilizing enzymes, engage in metal acquisition, and cross-feed or inhibit other microbiota effectively placing MOB at the confluence where diverse nutrient sources and cycles intersect. At the crux of MOB metabolism and nutrient cycling is copper as the crucial element enabling efficient methane oxidation, as

underscored by the redundant copper acquisition strategies ranging from utilizing an alternative MMO, copper hoarding via the MopE storage proteins to buffer against copper deficiency, and Mbn biosynthesis for copper scavenging and theft (Karlsen *et al.*, 2003, Johnson *et al.*, 2014). Thus, examining the copper deficiency response in MOB can yield valuable insights into their unique physiology and ecology regarding this critical element.

(2.9) *Methylomicrobium album* BG8

Methylomicrobium album BG8 (formerly *M. albus* BG8) is a fast-growing gamma-MOB that is an excellent model for examining MOB physiology in the context of nutrient cycling (Tays *et al.*, 2018, Sugden *et al.*, 2021). This bacterium has pMMO, but not sMMO, for methane oxidation (Yuan *et al.*, 1999), a calcium-dependent MxaF and a lanthanide-dependent XoxF for methanol oxidation to formaldehyde, it assimilates formaldehyde primarily through the RuMP cycle, and encodes a molybdenum-dependent formate dehydrogenase that is utilized to oxidize carbon to CO₂ to generate reducing equivalents. Methane-grown *M. album* BG8 differentially expresses genes for ion transport, motility, and secondary metabolite synthesis when compared to methanol-grown cells (Sugden *et al.*, 2021). Although methanol alone is a sufficient carbon and energy source for *M. album* BG8, copper has been shown as a necessary growth factor despite not needing pMMO in the absence of methane. As pMMO and MeDH enzymes are co-localized as a complex, *M. album* BG8 is classified as an obligate methanotroph (Brantner *et al.*, 1997). *M. album* BG8 grown solely on methanol has more abundant fatty acids, phospholipids, and aromatic and branched-chain amino acids as observed from transcriptomic and metabolomic analysis (Sugden *et al.*, 2021). While fatty acid methyl ester analysis indicated a change in fatty acid composition primarily between methane- versus methanol-grown cells, no significant difference in the total abundance of lipids was observed between different carbon or nitrogen sources. Methanol also stimulated sugar catabolism and increased ribosome biogenesis (Sugden *et al.*, 2021), as methanol bypasses pMMO catalysis, the rate-limiting step in methane oxidation. Providing *M. album* BG8 with methanol as the sole carbon source activated stress-related genes, such as those for the stress-response sigma factor *rpoE*, carbon storage,

oxidative stress, and genes related to glutathione-dependent formaldehyde detoxification, with lower abundance of gamma-glutamyl amino acids, 5-oxoproline and glutamate, indicating active use of the formaldehyde detoxification pathway. In *M. album* BG8, pMMO has been shown to oxidize ammonia to toxic hydroxylamine that is further detoxified via its native hydroxylamine oxidoreductase (HaoAB) to produce nitrite (Nyerges *et al.*, 2010). Ammonia oxidation was demonstrated as a source of reducing potential when *M. album* BG8 was placed under oxygen limitation with supplemented nitrite, although the cells were not capable of growing from ammonia oxidation (Kits *et al.*, 2015). *M. album* BG8 increased expression of the lesser characterized *pmoA* homolog *pxmA* under hypoxia in the presence of nitrate/nitrite. Under oxic conditions, *M. album* BG8 upregulates *haoAB* and overall metabolic activity when grown with ammonium and the N-source (Tays *et al.*, 2018, Sugden *et al.*, 2021). Under methanol plus ammonium conditions, carbon flux is upregulated in the Embden-Meyerhof-Parnas (EMP), pentose phosphate (PP), and partial serine cycle pathways, whereas nitrate decreases carbon flow into the Entner-Doudoroff pathway (Tays *et al.*, 2018, Sugden *et al.*, 2021). A lowered metabolic activity observed with methanol plus nitrate may be due to a potential bottleneck in the PP pathway, as *M. album* BG8 accumulates xylitol, presumably derived from xylulose-5-phosphate. The activation of central metabolic pathways with either carbon source and ammonium corresponds with observations of enrichment of gamma-MOB in rice paddies (Chang *et al.*, 2021). How copper deficiency affects ammonia co-metabolism is less studied, but presumably copper-deficiency could affect the metabolism of different nitrogen sources by *M. album* BG8, as the lack of pMMO would decrease ammonia co-metabolism.

M. album BG8 responds to short-term methane and oxygen limitation not unlike how it responds to the type of available carbon or nitrogen source; in brief, *M. album* BG8 reconfigures its central metabolic pathways and its electron transport chain (ETC) while upregulating genes relating to chemotaxis, motility and conjugation (Tentori *et al.*, 2022). *M. album* BG8 upregulates the PP pathway more strongly in response to methane limitation and downregulates the EMP pathway less strongly. Differential expression of the ETC is mixed with NADH oxidoreductase and cytochrome genes upregulated in response to methane limitation. Oddly, MxaF was downregulated and XoxF was upregulated with methane limitation despite no

change in lanthanide availability, suggesting a role in stress response for XoxF. One possible explanation in the change of MeDH expression is an attempt to shunt carbon towards formate for generating reducing potential. Overall, the response to methane limitation was stronger than that to oxygen-limitation (Tentori *et al.*, 2022). *M. album* BG8 and similar MOB have been demonstrated to adapt to hypoxic conditions, and *M. album* BG8 shifts to utilizing its glycogen stores to maintain metabolism in response to methane limitation and upregulate its formate dehydrogenase to shunt carbon towards generating reducing potential over carbon assimilation. Upregulation of chemotaxis, motility, and conjugation is intuitive and corresponds to known bacterial responses to nutrient limitations (Wheeler *et al.*, 2019, Pison, 2023).

Copper is an essential nutrient to *M. album* BG8. Copper-starved cells were observed to be smaller in mass with less intracytoplasmic membrane, and the addition of copper reversed these effects (Brantner *et al.*, 1997). The addition of copper stimulated the formation of intracytoplasmic membrane, where pMMO and MeDH reside (Brantner *et al.*, 2002), leading to increased pMMO activity and cell yield (Collins *et al.*, 1991). Copper naturally accumulates on the surface of *M. album* BG8 (Berson & Lidstrom, 1996) via binding to a metalloprotein called CorA (Johnson *et al.*, 2014). Along with its copper-sensing partner CorB, CorA acts as copper storage protein with an important role in maintaining copper homeostasis, as *corA* is repressed when *M. album* BG8 is grown in sufficient copper and *corA* mutants exhibited stunted growth (Berson & Lidstrom, 1997). MopE, a CorA homolog from *Methylococcus capsulatus* Bath, is likewise found to fluctuate inversely in relation to copper levels on the cell surface and supernatant (Karlsen *et al.*, 2003). Taken together, CorA may be a “copper bank” by which *M. album* BG8 is able to rely on as a buffer to copper deficiency. While *M. album* BG8 has long been known to produce a metabolite with high affinity for binding copper, only recently was it spectrally characterized, confirming that *M. album* BG8 produces its own chalkophores (Kang-Yun *et al.*, 2022). Although *M. album* BG8 can produce its own native Mbn, low production of Mbn secreted into the supernatant has made structural characterization of the *M. album* BG8 Mbn difficult. A knock-out mutant of a putative *mbnT* (Metal_1282 aka Metal_RS06265) is capable in growing in low-copper media when Mbn from *Methylosinus trichosporium* OB3b or *Methylocystis* sp. SB2 is supplemented, indicating “theft” of foreign chalkophores as a competitive strategy to obtain copper (Kang-Yun *et al.*, 2022). Association of copper with biomass in the putative *mbnT* knockout is statistically similar between wildtype and *mbnT* knockouts. Methylmercury degradation via binding to Mbn – a measure of

Mbn activity and uptake into the cell – was not observed in *mbnT* knockouts. Mbn produced by *Methylocystaceae* have been directly observed to have a stronger binding affinity to copper and can take copper away from Mbn produced by *Methylococcaceae*, supporting the 'chalkophore theft' hypothesis (Choi *et al.*, 2010). Yet, *M. album* BG8 *mbnT* mutants grew well despite producing a chalkophore with weaker binding affinity to copper, indicating that *M. album* BG8 can competitively acquire copper for its own metabolism even without engaging in Mbn theft.

Although it can produce a chalkophore, the BGC encoding for the *M. album* BG8 Mbn has yet to be described. While a putative *mbnT* has been identified, multiple TonB transporter receptors have been identified in Mbn uptake (Peng *et al.*, 2022), thus confirmation of a copper-responsive BGC is necessary to validate a putative Mbn BGC. Identifying the putative Mbn BGC would aid in elucidating the structure of the *M. album* BG8 Mbn and enable identification of homologous BGCs in *Methylococcaceae* and comparison against *mbn* genes encoded in *Methylocystaceae*. Although *M. album* BG8 has stunted growth in copper depleted conditions, an overall copper starvation stress response has yet to be characterized at a system level. The in-depth analysis carried out in this thesis aims to tie together all the strategies that a pMMO-obligate gamma-MOB can employ to compete for copper in its environment, as well as reveal potentially uncharacterized avenues by which gamma-MOB respond to copper starvation stress.

(3) Methods

(3.1) Media preparation

M. album BG8 was cultured as previously described (Whittenbury *et al.*, 1970, Tays *et al.*, 2018, Sugden *et al.*, 2021, Kang-Yun *et al.*, 2022) in five biological replicates for each of 8 combinatorial conditions in 100 mL media placed into 250-mL Wheaton media bottles and sealed with butyl-rubber septa caps. Prior to the addition of media, the bottles were soaked twice in 3 M hydrochloric acid and rinsed in ddH₂O to minimize trace copper contamination. 10x concentrated nitrate mineral salts (NMS) and ammonium mineral salts (AMS) media were prepared using non-metallic elements, filtered through a Chelex-100 column (15 grams, Sigma Aldrich) to remove trace metal contaminants. Ferrous iron and trace metal solution was subsequently added. At working dilutions, the final concentration of both nitrogen sources (ammonium or nitrate) was 10 mM. Working solutions were sterilized via autoclave, and 1.5 mL of sterile phosphate buffer (26 g/L KH₂PO₄, 33 g/L Na₂HPO₄) was added to room-temperature media to buffer at pH of 6.8. Copper (CuSO₄) was added as needed in copper replete conditions to 10 μM, and none was added for copper deplete conditions. Finally, carbon sources were added at 2.5 mmol. For methane (99.9% purity), 50 mL of air was first withdrawn from the headspace and 60 mL methane was injected into the bottle via a 0.22-μm filter-fitted syringe. High performance liquid chromatography- (HPLC-) grade methanol was directly pipetted into sterile media.

(3.2) Culturing and growth measurements of *M. album* BG8

A first round of reducing residual copper was accomplished by inoculating 100 mL media with 1 mL *M. album* BG8 culture and grown to early stationary phase at an optimal temperature of 30°C with shaking at 150 rpm. The second round of cultures were inoculated and grown similarly with inoculum from the first round of growth. Optical density (OD) measurements were taken at 540 nm in 0.5-mL aliquots in a 48-well plate (Multiskan Spectrum, Thermo Scientific). Cell images were obtained under a transmission electron

microscope with a negative stain using 2% phosphotungstic acid (pH 7 – 7.4) and sized using ImageJ. 50 images were used per sample to determine the average diameter of cells grown under each nutrient condition. Cell dry weights were obtained by filtration of 100 mL stationary phase culture onto tared cellulose filters, dried at 90 °C overnight, and weighed. Gas chromatography (GC) measurements were conducted to measure oxygen, carbon dioxide, and methane in the gas headspace via a gas chromatograph (Shimadzu) equipped with molecular sieve 5A and Hayesep Q columns (Alltech). A 250 µL gas-tight syringe (SGE Analytical Science) was used to extract and inject 100 µL sample from the gas headspace of culture bottles onto GC columns at injection and column temperatures of 90 °C and 120 °C, respectively. 90 mA current was maintained through the thermal conductivity detector and 200 kPa helium carrier gas (Ultra High Purity, Praxair) was maintained.

(3.3) RNA extraction and transcriptomic analysis

RNA extraction from 3 biological replicates followed protocols previously established in the lab (Tays *et al.*, 2018). Cells were harvested for RNA extraction at log phase after 30 h growth for methane/copper replete replicates, 54 h for methane/copper deplete replicates, 60 h for methanol/copper replete replicates, and 70 h for methanol/copper deplete replicates as shown with black arrows in Figure 1 C-D. Cell cultures from each replicate were inactivated via a cold 5% phenol 95% ethanol stop solution, pelleted and concentrated to 10 mL, and then flash frozen with liquid nitrogen and stored at -80 °C for batch extraction. Samples were subsequently processed with the MasterPure RNA Purification kit (Epicentre) according to manufacturer instructions with an alteration of 0.35 mg proteinase K added to aid in lysing the cells. RNA samples were purified with a second RNA purification kit (Zymo Research) according to the manufacturer's instructions. RNA samples were quality checked using a Bioanalyzer (Agilent) and sequenced using Illumina-HiSeq by an external service provider (Genome Quebec). Raw reads were imported into Geneious R11, filtered via the BBDuk plugin for quality control, and mapped to the *M. album* BG8 genome (accessions: NZ_CM001475.1 chromosome, NZ_CM001476.1 plasmid). Principal component analysis (PCA) was conducted using the Sci-Learn kit available in the Anaconda distribution to

determine percent variance per nutrient condition. Differential expression was calculated using the DESeq2 plugin in Geneious and visualized in a Circos-style diagram via shinyCircos-v2.0 (Yu *et al.*, 2018). Gene set enrichment analysis (GSEA) was conducted using the online web server FUNAGE-Pro (de Jong *et al.*, 2022), a GSEA algorithm tailored specifically for prokaryotes. Genome annotations from NCBI were cross-referenced with UniProtKB entries to confirm identity and function.

(3.4) Bioinformatic analyses of biosynthetic gene clusters

A variety of BGC detecting software was employed to predict BGCs by type and function within the transcriptome dataset. antiSMASH v6.1.1 (Blin *et al.*, 2021), DeepBGC v0.1.23 (Hannigan *et al.*, 2019), GECCO v0.9.6 (Carroll *et al.*, 2021) and FeGenie v1.2 (Garber *et al.*, 2020) were used to calculate sequence similarity and categorize BGCs against their internal databases and MIBiG database of known BGCs. BiG-SCAPE was employed to conduct a network and phylogenetic analysis of BGCs (Navarro-Munoz *et al.*, 2020). Reference genomes were obtained from the class *Methylococcaceae*, as well as reference genomes from all bacterial phyla with known curated BGCs within the MIBiG 3.1 repository (Terlouw *et al.*, 2023), including members of the *Proteobacteria*, *Cyanobacteria*, *Actinobacteria*, *Bacteroidetes*, *Chloroflexi*, *Verrucomicrobia*, *Firmicutes*, *Candidatus Tectomicrobia* and *Planctomycetes*. A database of genomes was built using cblaster to identify homologous co-occurring genes corresponding to BGCs in *M. album* BG8 (Gilchrist *et al.*, 2021). Identified regions were downloaded from NCBI and processed via antiSMASH for BGC detection. antiSMASH outputs were inputted to BiG-SCAPE v1.1.5 to align putative BGCs with *Methylococcaceae* homologs and known MIBiG BGCs by aligning functional domains using PFam HMMs with “glocal” settings and cutoffs set at the maximum exploratory threshold of 1.0 (Navarro-Munoz *et al.*, 2020).

The methodology described in RiPPER was used to generate a phylogenetic tree using a ‘bait’ protein (Santos-Aberturas *et al.*, 2019). Although it was suggested to use tailoring enzymes identified by RODEO (Tietz *et al.*, 2017) that are known to be involved in the maturation of the RiPP precursor peptide, tailoring enzyme candidates were not used as none were recognized by RODEO. The candidate enzymes

had other drawbacks as well; DNA-methyltransferase (Metal_RS21020) was too small for quality resolution, and only 4 known bacterial BGCs from MIBiG (Terlouw *et al.*, 2023) contained a similar penicillin amidase/acylase family protein, thus making phylogenetic inferences difficult from the lack of curated data. Therefore, cyclic peptide export type ABC transporter (Metal_RS13165) was selected for phylogenetic analysis instead, as previous studies have revealed the sequence/structure of such transporters can be correlated to their function (Dassa & Bouige, 2001). An InterPro scan of Metal_RS13165 was used to inform the domains present in the transporter, revealing the entry IPR005898, and contained within were sub-entries IPR011527 and IPR03439. Bacterial reference proteins with combined InterPro entries IPR005898, IPR011527, and IPR03439 were retrieved from UniProtKB. Transporters from BGC sequences obtained from MIBiG were filtered only with IPR00585 to preserve a higher number of curated BGC hits for phylogenetic analysis. Accession IDs were processed for network analysis via the EFI-EST (Gerlt *et al.*, 2015) tool and filtered at 95% identity to remove identical proteins. Representative proteins were retrieved from NCBI and aligned using MUSCLE (Edgar & Soc, 2004) with the output used as the input to generate a RAxML phylogenetic tree visualized and trimmed in iTOL (Stamatakis, 2014, Letunic & Bork, 2016). Mbn precursor candidates for *M. album* BG8 were obtained via the RODEO and Prodigal-short modules contained in RiPPER v.1.1, and searched via the NLPPrecursor module in the DeepRiPP web tool (Merwin *et al.*, 2020) as well as the RiPPMiner webtool for RiPP classification (Agrawal *et al.*, 2017). Structural similarity searches in the Natural Product Atlas (NPAtlas) database (van Santen *et al.*, 2021) were conducted with a lowered threshold of 0.5 via input of their predicted Simplified Molecular-Input Line-Entry System (SMILES) notation and visualized in MolView. Corresponding regions of *M. album* BG8 Mbn precursor in closely related MOB were searched utilizing NCBI ORF Finder to scan for minimal ORF lengths of 30 nucleotides using genetic code 11 for any sense codon, aligned using MAFFT (Kato & Standley, 2013), and visualized using Jalview (Waterhouse *et al.*, 2009).

(4) Results

(4.1) Copper deficiency stunts growth of *M. album* BG8

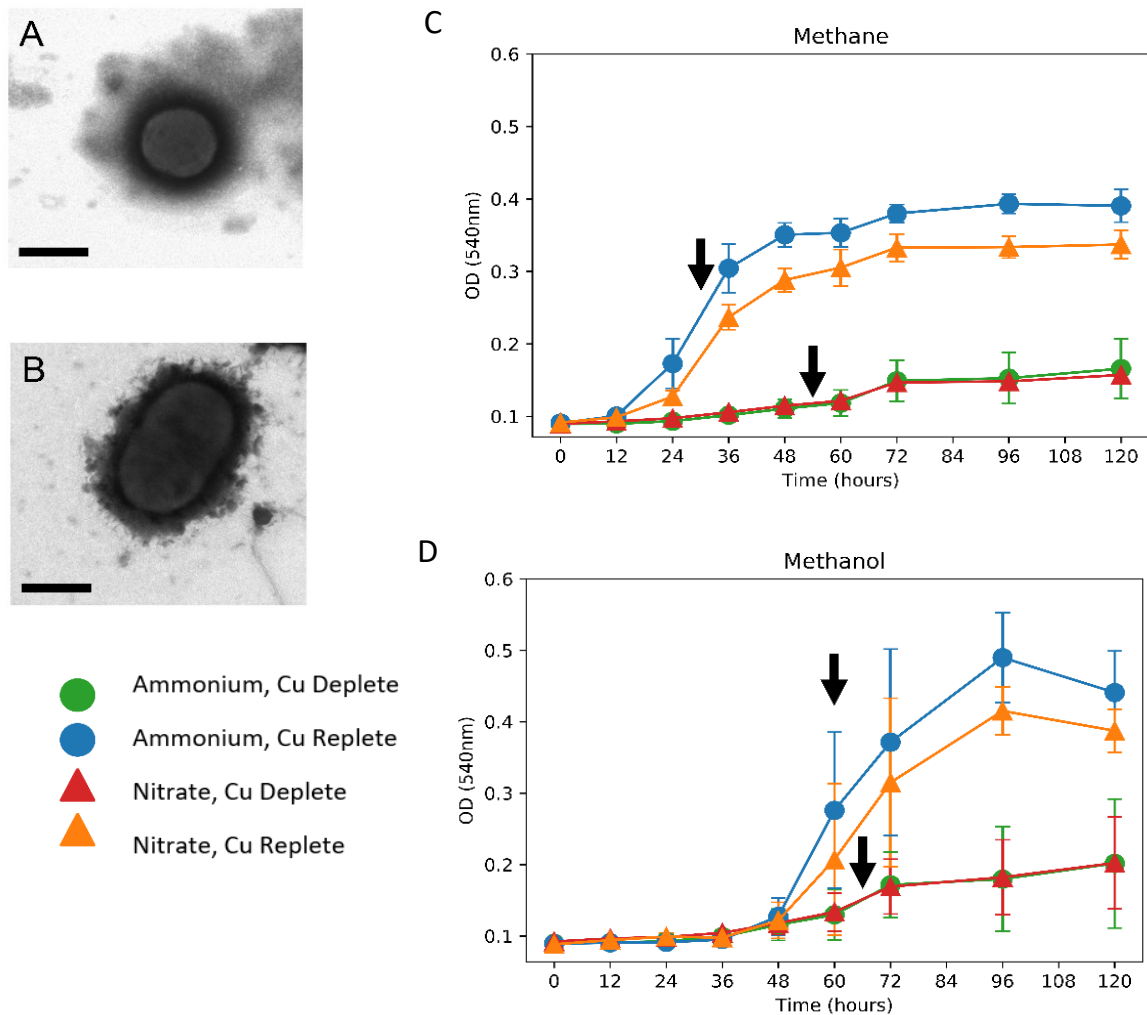


Figure 1. Cell morphology and growth of *M. album* BG8. TEM images of cells grown in (A) copper depleted vs (B) replete conditions, black bar = 1 μm . Optical density (540nm) growth curves of a total of 8 combinatorial nutrient conditions were plotted according to carbon source (C) methane or (D) methanol, with either nitrogen: nitrate or ammonium, and copper: replete or depleted conditions (n=5). Black arrows indicate the time cells were harvested for RNA extraction. Error bars represent 95% confidence intervals.

Methylomicrobium album BG8 was grown in copper-free media for depleted conditions, with copper supplementation (10 μ M) for copper replete conditions. *M. album* BG8 cells shrunk in size under copper starvation and exhibited a round morphology (Figure 1A) as opposed to when grown in copper replete conditions (Figure 1B). The shrinkage in morphology was observed across all copper depleted conditions, and cell sizes were significantly smaller for all conditions when grown without copper except when grown with methane and nitrate (Appendix Figure 1). Growth curves of *M. album* BG8 indicated stunted growth under copper depleted conditions; however, cultures fed with methanol had increased variability in growth as cultures did not enter logarithmic growth synchronously to those fed with methane. GC measurements expectedly corresponded to growth trends observed in the OD measurements, with methane and oxygen consumed and carbon dioxide generated over time, suggesting little effect of carbon and nitrogen source on methane oxidation (Appendix Figure 2).

(4.2) Transcriptome reveals a uniform, selective, copper starvation response

Sequenced mRNA reads were analyzed in Geneious R11 with differential expression values calculated using DESeq2. The PCA of averaged read counts across biological triplicates revealed a percent variance of 59.1% for PC1, 17.8% for PC2, and 9.4% for PC3, suggesting copper availability had by far the strongest influence on gene expression, followed by the type of carbon source (methane or methanol) and lastly nitrogen source (ammonium or nitrate) (Appendix Figure 3). Copper depleted gene expression datasets converged into a tight cluster, as compared to their copper repleted counterparts, implying the overall stress response was similar regardless of the carbon and nitrogen sources provided. Since carbon and nitrogen had little effect on the copper stress response, the transcriptome datasets were subsequently

collapsed into two based on copper availability, and differential expression values were calculated with all copper depleted conditions against all copper replete conditions.

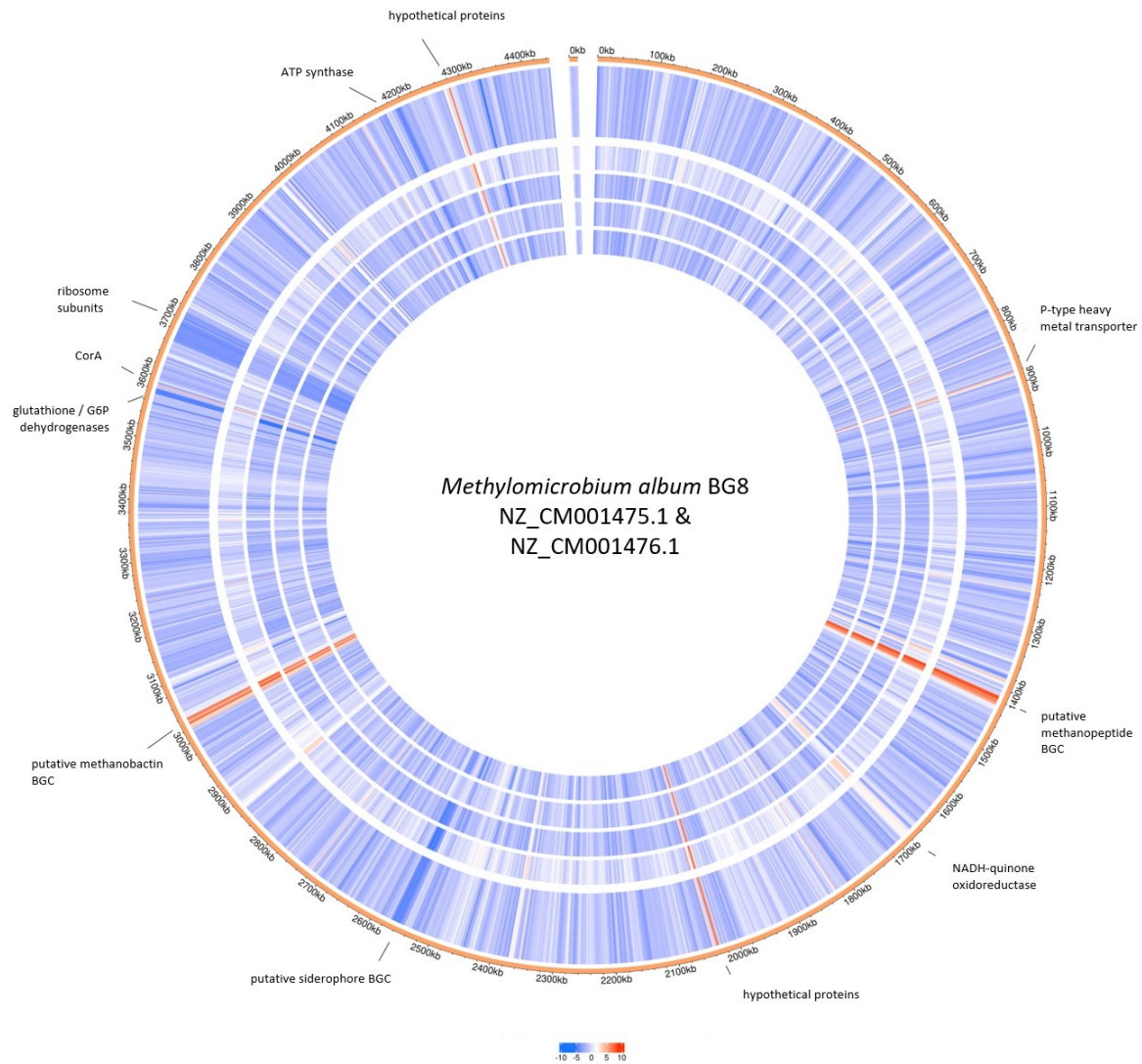


Figure 2. Heatmaps of differentially expressed genes of *M. album* BG8 chromosome and plasmid. The large outermost heatmap ring are Log₂ ratios of fold change from all copper depleted vs replete nutrient conditions. Moving inward from the second outermost ring are copper depleted vs replete conditions in: nitrate and methane, ammonium and methane, nitrate and methanol, and ammonium and methanol.

Heatmaps of all copper depleted vs all copper replete conditions, combined or otherwise, showed that the copper starvation response was similar for all conditions (Figure 2), although differential expression of transcripts was less affected by copper starvation when *M. album* BG8 was grown in nitrate and methane

relative to the other nutrient combinations. Genes for pMMO (Metal_RS06970, Metal_RS06975, Metal_RS06980) did not show differential expression, however the homologous pXMO gene cluster (Metal_RS017420, Metal_RS017425, Metal_RS017430) showed slight downregulation under copper depletion. The MxaF (Metal_RS06790) MeDH was moderately upregulated in ammonium, and downregulated in nitrate, whereas XoxF (Metal_RS11970) was not differentially expressed under copper depletion. One out of three formaldehyde activating enzymes in *M. album* BG8 was upregulated (Metal_RS7310) under copper depletion. Overall, GSEA of *M. album* BG8 suggested a shutdown of general metabolism, with areas of strong upregulation of a few gene clusters under copper depletion. GSEA conducted on the pan-copper depleted vs repleted values showed downregulation in the synthesis of essential protein machinery such as ATP synthase (GO:0046933, GO:0045261, GO:0045263), ribosomes (GO:0005840, GO:0015934, GO:0015935, GO:0019843), and translation (GO:0006412) (Appendix Figure 4). NADH dehydrogenases and quinones (GO:0050136, GO:0048038) were upregulated to maintain a pool of reducing equivalents, possibly less for ATP generation (as ATP synthases were downregulated), but rather for the biosynthesis of secondary metabolites as indicated by differential expression of genes related to peptide transmembrane transport (GO:1904680) and antibiotic biosynthesis (GO:0017000) under copper depletion. The overarching trend for the copper starvation response was for *M. album* BG8 to primarily downregulate genes related to energy production and conversion (COG: C), while also downregulating translation, ribosomal structure, and biogenesis (COG: J) functions.

While metabolism was downregulated, there were select genes intensively upregulated across all carbon and nitrogen combinations with copper depletion (Figure 2, Appendix Figure 5). Upregulation in transcriptional regulators such as a sigma-70 family RNA polymerase sigma factor (Metal_RS07995) and TraR/DksA family transcriptional regulator (Metal_RS03395) suggest their involvement in a targeted stress response. CorA (Metal_RS15600) – a copper binding protein homologous to MopE from *Methylococcus capsulatus* Bath and regarded as a copper storage protein – was upregulated (Karlsen *et al.*, 2003, Johnson *et al.*, 2014), as well as a P-type heavy metal transporter (Metal_RS20450) homologous to known copper transporters.

Three predicted BGCs were differentially expressed, of which two were detected by all three BGC detection algorithms, whereas the third was only detected by DeepBGC (Figure 3) (Hannigan *et al.*, 2019). Boundaries for each predicted cluster varied greatly, as upstream genes often contain regulatory proteins in BGCs, and neighboring genes are known to frequently contain HMM profiles indicative of biosynthetic activity. The boundaries of differentially expressed BGCs indicated by the transcriptome were mostly, if not entirely, contained within the ranges predicted by antiSMASH (Blin *et al.*, 2021), DeepBGC, and GECCO (Carroll *et al.*, 2021). Two BGCs were categorized as encoding for an NRP, and the third a RiPP. Other detected BGCs did not show significantly differential gene expression under copper depletion.

(4.3) Analysis of three differentially expressed biosynthetic gene clusters and their natural products

Figure 3A represents the heatmap of loci in the BGC with the highest fold change in gene expression under copper depletion, Metal_RS06240, which is annotated as an ankyrin repeat domain-containing protein with a Log base 2 value of 9.34 (~650 fold) and nearby NRPS modules expressed with similar values. A cluster blast search with cblaster (Appendix Figure 6A) indicates 5 core biosynthesis modules (Metal_RS6230/ WP_245549480.1, Metal_RS6245/ WP_245549481.1, Metal_RS6250/ WP_005370688.1, Metal_RS6255/ WP_005370690.1, and Metal_RS6260/ WP_005370697.1). Searching against the antiSMASH database via the KnownClusterBlast algorithm returned a closest hit of low sequential similarity to the endopyrrole (BGC0002048) BGC in *Mycetohabitans rhizoxinica* for triggering bacterial-fungal endosymbiosis with the fungi *Rhizopus microsporus* (Niehs *et al.*, 2019). antiSMASH's

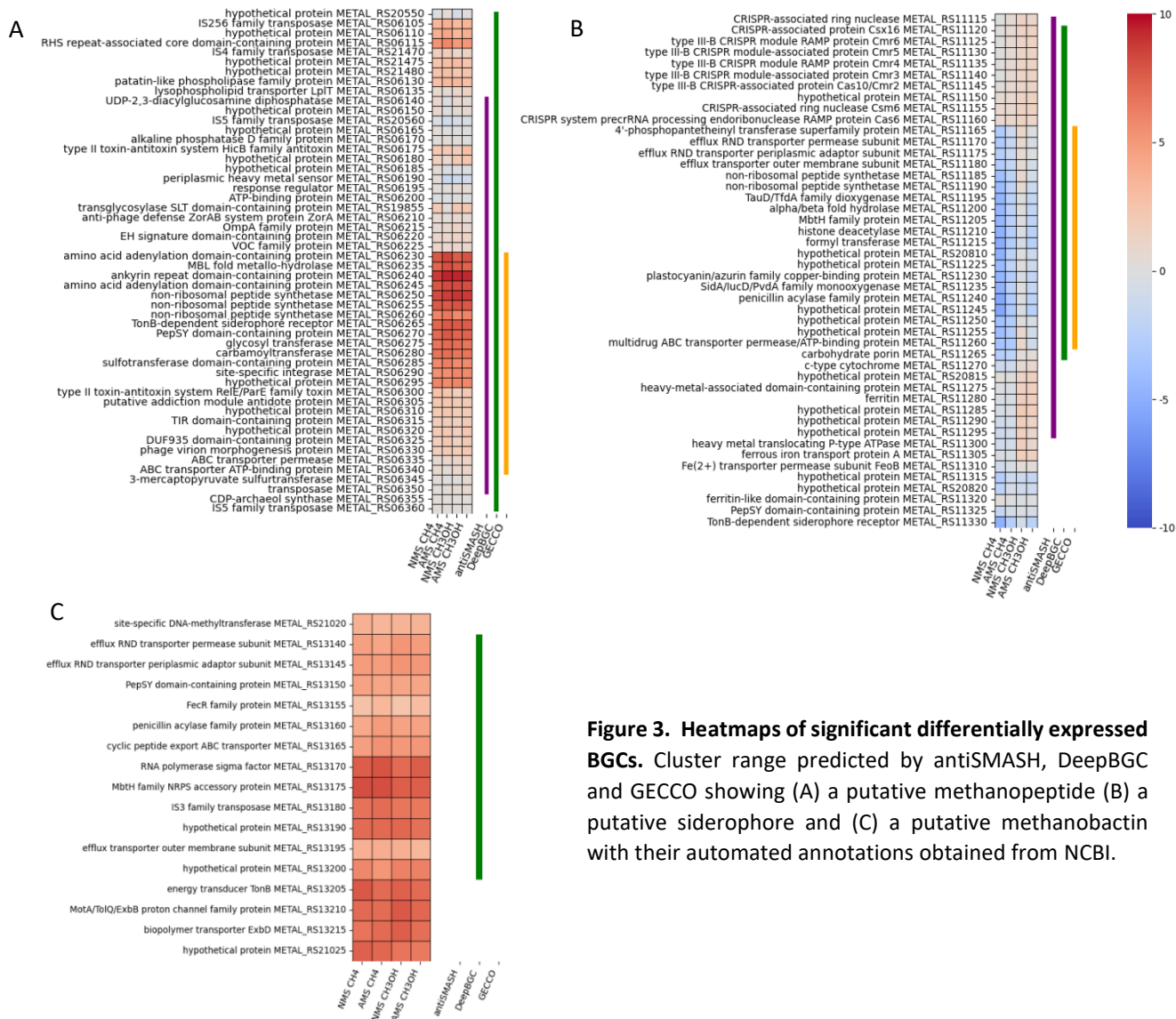


Figure 3. Heatmaps of significant differentially expressed BGCs. Cluster range predicted by antiSMASH, DeepBGC and GECCO showing (A) a putative methanopeptide (B) a putative siderophore and (C) a putative methanobactin with their automated annotations obtained from NCBI.

MiBIG comparison module returned hits on “antimicrobial” NRPs including those encoded from the symbiotic genera *Pseudomonas* (Cusano et al., 2011), *Paraburkholderia* (Mather et al., 2023), and *Xenorhabdus* (Chaston et al., 2011). BiG-SCAPE (Navarro-Munoz et al., 2020) alignments indicated similar putative BGCs detected in *Methylococcaceae* by antiSMASH form their own distinct clade when compared to curated BGCs from MIBiG, indicating potential functions specific to members of *Methylococcaceae* (Appendix Figure 7A). Contrary to the antiSMASH results, the closest phylogenetically related clade of curated BGCs aligned to functional domains in BiG-SCAPE was that of products produced by cyanobacteria. These BGCs produce cyanopeptolin (BGC0000331) (Itou et al., 1999), micropeptin K139

(BGC0001018) (Nishizawa *et al.*, 2007), nostocyclopeptide A2 (BGC0000397) (Jokela *et al.*, 2010, Herfindal *et al.*, 2011), and anabaenopeptins (BGC0002512, BGC0000301) (Christiansen *et al.*, 2011, Saha *et al.*, 2020). Cyanopeptides are generally regarded as 'toxic' as cyanopeptides are largely related to the hepatotoxin microcystin (MC) which is produced at the height of cyanobacterial blooms (Bischoff, 2001). Although MC was not clustered with the *M. album* BG8 homolog – hereby termed “methanopeptide” (Mpt) – in BiG-SCAPE, a cluster of microcystin-dependent proteins (Zilliges *et al.*, 2011) were found to be upregulated in *M. album* BG8 under copper depleted conditions (Metal_RS10355, Metal_RS10365, Metal_RS10370).

There is ample evidence that the second identified BGC produces a siderophore centered around two NRPS (Metal_RS11185 and Metal_RS11190). This BGC was downregulated under copper depleted conditions, except no differential expression was found when *M. album* BG8 was grown with methanol and nitrate (Figure 3B). Upstream of the putative siderophore-BGC are CRISPR-associated proteins unlikely to be part of the same BGC, but they were included in both antiSMASH and DeepBGC predictions. antiSMASH's KnownClusterBlast returned hits to siderophore-producing BGCs from its internal database. However, comparisons to MIBiG revealed some similarity to 'antimicrobial' NPs along with siderophore BGCs from symbiotic genera such as *Xenorhabdus*, *Pseudomonas*, *Rhodococcus* (Dotson *et al.*, 2003), and *Azotobacter* (Monib *et al.*, 1979). A fourth algorithm, the siderophore-specific FeGenie (Garber *et al.*, 2020), returned significant hits on NRPS (Metal_RS11185 and Metal_RS11190) as Vab-F family siderophore synthases from vanchrobactin (BGC0000454) produced by *Vibrio anguillarum* RV22 (Balado *et al.*, 2006). From aligning conserved HMMs of BGCs, BiG-SCAPE indicated the siderophore to be related to pyoverdine SMX-1 (BGC0002693) from *Pseudomonas* sp. SXM-1 (Appendix Figure 7B) (Matthijs *et al.*, 2016). Plantaribactin (BGC0002565) from *Burkholderia plantarii* (Hermenau *et al.*, 2019) and histocorrugatin (BGC0002422) from *Pseudomonas thivervalensis* (Matthijs *et al.*, 2016) were the next two closest related siderophores predicted by MIBiG. Lastly, while Metal_RS11260 and 2 other homologues from *Methylococcaceae* formed their own clade, phylogenetic analysis of homologous ABC type transporters across the domain *Bacteria* revealed that the clade is nested within a greater branch of ABC transporters belonging to siderophore-producing BGCs, further supporting an iron scavenging function (Figure 4).

The third putative BGC in *M. album* BG8 was categorized as a RiPP and was only detected by DeepBGC. A cluster BLAST search with cblaster indicated that a cyclic peptide type ABC transporter (Metal_RS13165/ WP_005373037.1), a penicillin amidase/acylase family protein (Metal_RS13160/ WP_005373036.1), a FecR (Metal_RS13155/ WP_005373034.1), an RNA polymerase sigma factor (Metal_RS13170/ WP_005373040.1), and a MbtH family NRPS accessory protein (Metal_RS13175/ WP_005373041.1) were conserved in similar putative BGCs from some members of *Methylococcaceae* and likely form the core biosynthetic genes involved in the synthesis of this RiPP (Appendix Figure 6B).

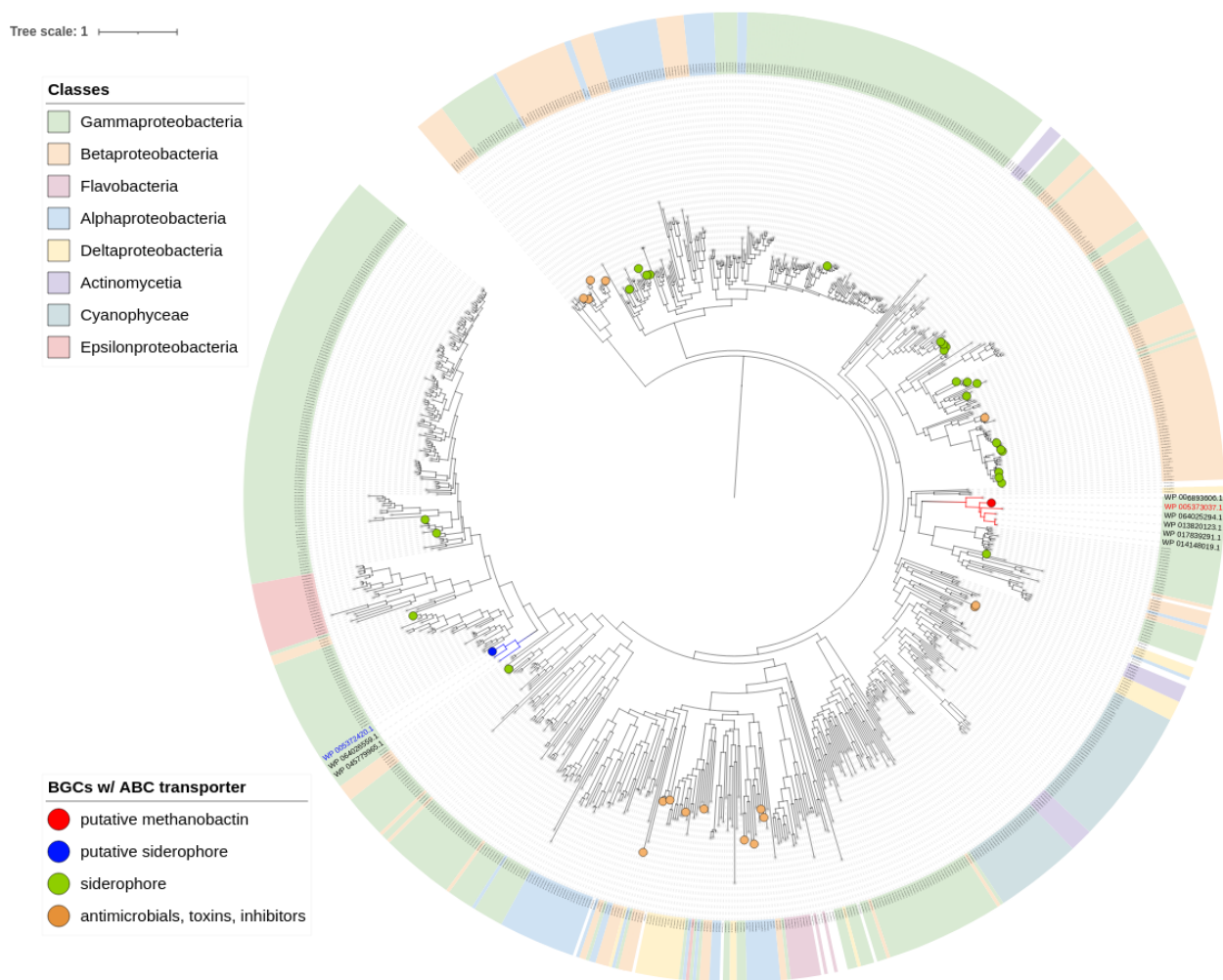


Figure 4. Phylogenetic tree of cyclic peptide type ABC transporters from the domain *Bacteria*. The outer ring of accession identifiers is color coded according to taxon class, with accession identifiers from *Methylococcaceae* enlarged and *M. album* BG8 identifiers highlighted. Transporters from known BGCs obtained from MIBiG repository are categorized by two product types: siderophores (green) and antimicrobials/toxins/inhibitors (orange).

The RODEO module in RiPPER did not recognize the BGC as a RiPP and only recognized the ABC-type transporter as evidence of a BGC. Therefore, Metal_RS13165 was integrated into the same phylogenetic analysis as Metal_RS11260 from the siderophore-BGC, with Metal_RS13165 its own clade along with homologs from *Methylococcaceae* (Figure 4). The nearest related BGC in that branch with an ABC type transporter is known to produce histicorrugatin, a siderophore with 8 amino acids with an attached octanoic acid; albeit histicorrugatin is synthesized from NRPS modules (BGC0002422) (Matthijs *et al.*, 2016). Nearby are members of ABC type transporters belonging to *Cyanophycaceae*, however none of the transporter genes were matched to BGCs submitted to MIBiG. As a result of RODEO not recognizing the RiPP BGC, a sequence similarity network analysis of precursor peptide candidates generated by RODEO and RiPPER's Prodigal-short module was not automatically launched. Instead, precursor candidates from *M. album* BG8 were inputted into RiPPMiner's Class Prediction module and DeepRiPP's NLPPrecursor module. Although RiPPMiner did not identify a precursor peptide from candidates obtained from RiPPER, DeepRiPP's NLPPrecursor module (Merwin *et al.*, 2020) annotated a small peptide encoded upstream of the ABC transporter (Metal_RS13165) as a precursor peptide for a lassopeptide type RiPP. A manual search via NCBI ORF Finder and MAFFT alignment revealed a homologous peptide present in the same region within *Methylomicrobium* and closely related *Methylotuvimicrobium* (Appendix Figure 8). RiPPMiner's Cleavage and Crosslinks Prediction module returned three predicted model RiPPs under "lassopeptide" settings, with modest similarities to secondary metabolites from microbes found in extreme environments or engaged in symbiosis such as *Streptomyces*' sungsanpin in deep-sea sediments (Um *et al.*, 2013), chaxapeptin from the Atacama Desert (Elsayed *et al.*, 2015), burhizin from the endosymbiont *Mycetohabitans* (Bratovanov *et al.*, 2020), and the cyanobactins cyanothecamide and anacyclamide from *Cyanothece* and *Anabaena* (Martins & Vasconcelos, 2015). A similarity search in NPAtlas returned hits of modest structural similarity to burhizin and the antimicrobial surugamide from a halophilic *Streptomyces* found on preserved fish from Japan (Matsuda *et al.*, 2019).

(5) Discussion

While the copper starvation response of MOB encoding both pMMO and sMMO is controlled by a well characterized “copper switch” through regulator and repressor proteins to alter metabolic flux (Knapp *et al.*, 2007, Semrau *et al.*, 2013, Farhan UI Haque *et al.*, 2015), the copper starvation response in a pMMO-obligate gamma-MOB is instead one of metabolic shutdown. This response appears less refined when compared to the “copper switch”, but it nevertheless is selective for specific genes and BGCs that can be upregulated hundreds of folds. The downregulation of the putative siderophore-BGC, despite siderophores having some binding affinity towards other metals including copper (Koh & Henderson, 2015), implies an evolutionary selection towards utilizing NPs with better binding affinity to copper under copper starvation stress. Of the two BGCs that was intensively upregulated in response to copper starvation, the RiPP-producing BGC, is a convincing candidate to encode for the putative Mbn that has been detected in *M. album* BG8 (Kang-Yun *et al.*, 2022).

(5.1) The case for a cyanobactin-like methanobactin

The precursor peptide MbnA from canonical *Methylocystaceae* Mbn belongs to the linearazole-containing peptide group of RiPPs (Semrau *et al.*, 2020). The highly upregulated BGC in *M. album* BG8 is also predicted to belong to the lassopeptide subgroup of RiPPs. While research on lassopeptides have primarily focused on their antimicrobial activities, there are suggestions that lassopeptide BGCs are part of metal trafficking systems akin to that of siderophores due to their notable co-localization with downstream Fecl/R family proteins and isopeptidase. A proposed mechanism by which a lassopeptide releases its metal cargo is through a downstream, co-occurring isopeptidase hypothesized as being involved in cleaving the lasso ring to release a captured metal ion (Maksimov & Link, 2013, Maksimov *et al.*, 2015, Fouque *et al.*, 2018).

Furthermore, neighboring genes to BGCs tend to be functionally linked. To acquire copper, chalkophores must first be exported out of the cell. Nearby genes for RND family transporter subunits

(Metal_RS13140, Metal_RS13145) for efflux of secondary metabolites were also significantly upregulated, hinting to their involvement in an export function. As for import, a set of adjacent, highly upregulated genes encoding for TonB-ExbB-ExbD transporter complexes (Metal_RS13205, Metal_RS13210, Metal_RS13215) are located on the opposite flank of the core biosynthetic genes to the RND modules. The import of Mbn also requires a corresponding TonB-dependent transporter complex (TBDT). A significantly upregulated gene for an outer membrane receptor protein (Metal_RS13195) in-between the core biosynthetic genes and the TonB complex may be a potential candidate for reuptake of indigenous Mbn as the TBDT utilized for foreign Mbn import resides within the Mpt-BGC (Metal_RS06265).

Lastly, the putative Mbn BGC may not produce a lassopeptide as predicted. NP similarity searches of the putative methanobactin returned hits to cyanobactins, of which some are known to act as chalkophores that bind copper. One such cyanobactin is patellamide D (aka ascidiacyclamide), one of a series of cyclic pseudo-octapeptides produced by *Prochloron didemni*, an obligate marine cyanobacterial endosymbiont partner to the ascidian (sea squirt) *Lissoclinum patella* (van den Brenk *et al.*, 1994, Schmidt *et al.*, 2005). Patellamide D and its derivatives bind primarily to copper (II), and to a lesser extent zinc (II). Patellamide D binds via Lewis acid/base interactions to two Cu(II) ions coordinated by three nitrogen atoms from two azolines and an amide, with a carbonate bridge in-between the two Cu(II) ions (van den Brenk *et al.*, 1994). Downstream of a universal threonine recognition site for maturation machinery, the *M. album* BG8 putative Mbn precursor has a conserved, C-terminal region of hydrophobic residues (Appendix Figure 8), with the smallest predicted cyclized heptapeptide coinciding with this region (Figure 5A, Core Peptide 3). Speculatively, a similar coordination of Cu(II) ions to patellamide may also apply to *M. album* BG8 Mbn where a cyclized VFFKAGD heptapeptide with seven amide nitrogen atoms and one lysine R-group nitrogen atom would coordinate with two Cu(II) and also bridged with a carbonate, rendering the internal complex of coordinating ligands (Lewis base) and copper ions (Lewis acid) electronegatively neutral and forming a “saddle” configuration similar to that described for Cu(II)-bounded patellamide (Figure 5B). Unlike

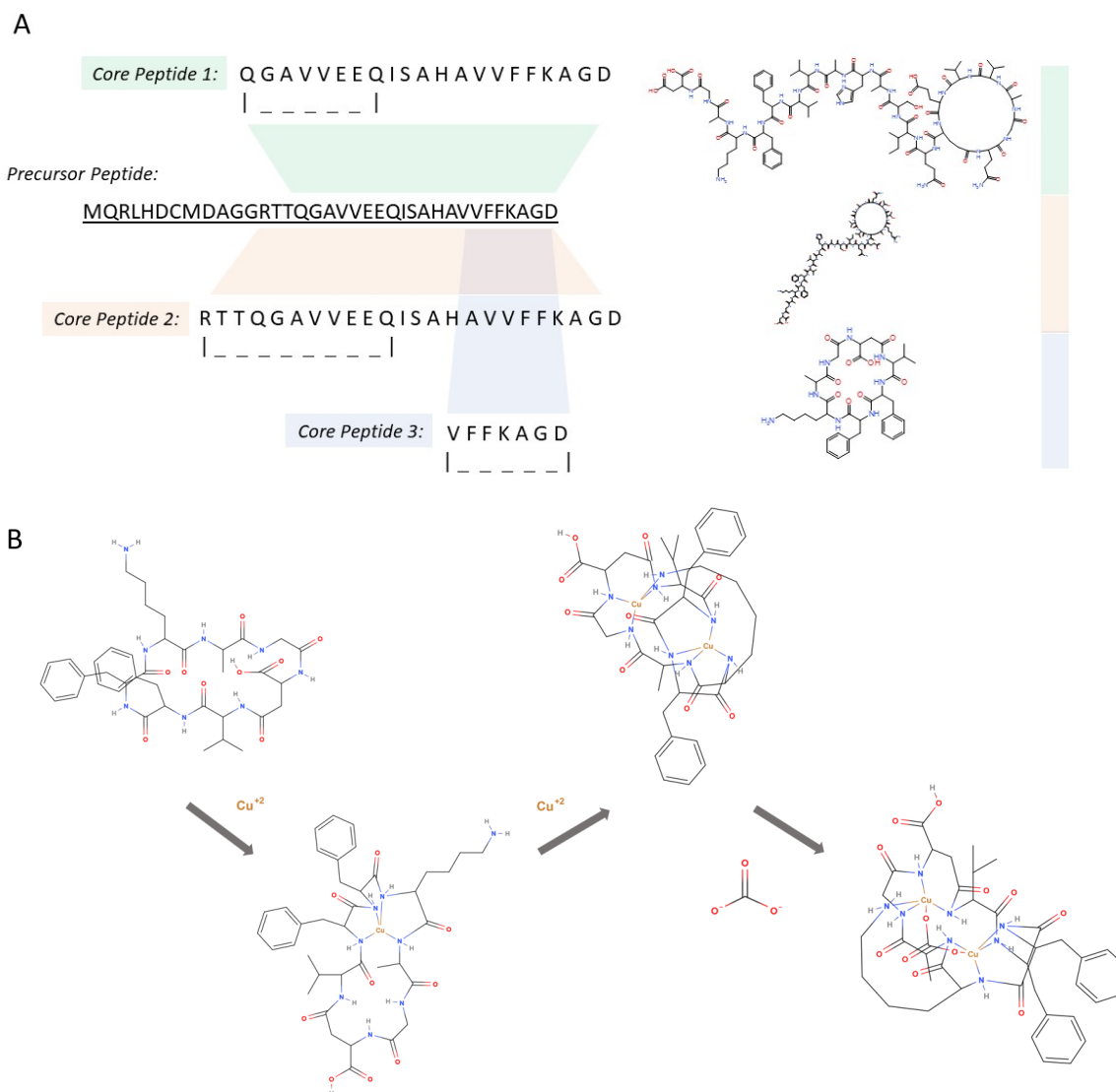


Figure 5. Putative peptide structure of novel methanobactin. (A) Predicted models from RiPPMiner of potential lasso-peptides derivable from putative precursor peptide and their predicted structures, and (B) proposed binding mechanism of putative methanobactin using smallest predicted core peptide with two copper(II) ions and carbonate.

patellamide (and canonical Mbn) containing azol(in)e heterocycles, cyclodehydratases that can form heterocycles in the putative Mbn are absent from the BGC. BLASTp results reveal that Metal_RS13170 has some sequence similarity to Fecl along with cysteine protease activity motifs detected via the MEROPS peptidase database (Rawlings *et al.*, 2018), suggesting a RiPP recognition element/leader peptide protease protein hybrid as seen previously involved in the maturation of some lasso-peptides. That leaves penicillin amidase family protein (Metal_RS13160) as likely responsible cyclizing the N and C terminus of the core

peptide, leaving a lack of obvious tailoring enzyme candidates except for an accessory methyltransferase (Metal_RS21020) that could introduce chemical alterations post-cyclization.

(5.2) Inferring the function of novel "methanopeptide"

The upregulated expression of a "methanopeptide" (Mpt) in *M. album* BG8 with homology to cyanopeptides – a class of peptides generally regarded as toxic enzyme inhibitors (Egli *et al.*, 2020) – reveals a novel actor involved in the copper starvation response of this and, potentially, other MOB. The few publications on BGCs with homology to the Mpt of *M. album* BG8 focus mainly on bioactivity in a medical context. Cyanopeptolins (previously aka 'oscillapeptins') are serine protease inhibitors, and along with micropeptin K139, have activity against pancreatic proteases (Itou *et al.*, 1999, Nishizawa *et al.*, 2007). The best researched cyanopeptides listed is nostocyclopeptide A2, an antitoxin to the well-researched microcystin (MC) toxin that functions by inhibiting uptake transporters found on hepatocyte cells membranes (Jokela *et al.*, 2010, Herfindal *et al.*, 2011).

Inferring the purpose of Mpt by comparison to cyanopeptides is problematic as *a)* their numerous variations in NRPS modules and tailoring enzymes within the same class results in enormous diversity in product structures with differing functions, *b)* there is often minimal research beyond enzyme activity assays and biochemical characterizations, and *c)* there is a lack of consensus on the role of cyanopeptides at the height of cyanobacterial blooms (Welker & von Dohren, 2006, Pineda-Mendoza *et al.*, 2016, Natumi & Janssen, 2020). However, some clues point toward a likely hypothesis. The presence of the TBDT *mbnT* homolog (Metal_RS06265) within the Mpt-BGC suggests a function associated with Mbn theft. Given some closely related BGCs produce cyanopeptides with serine protease inhibiting activity, Mpt may simply be an inhibitor against proteases that degrade Mbn to release their bound copper, thereby protecting unbound Mbn or cellular components from proteolysis. The presence of copper-bound Mbn may then repress Mpt production to restore proteolytic activity of the protease to free the bound cargo. However, this hypothesis has some caveats, as it presumes canonical or indigenous Mbn requires a protease to release its copper cargo, and this mechanism has yet to be described. Both Mpt and Mbn BGCs encode for a protein with a

PepSy domain (Metal_RS06270, Metal_RS13150) known for protease inhibition (Yeats *et al.*, 2004), making them alternative candidates for this purpose as well. Examining the varied roles of cyanopeptides suggests other possible purposes for Mpt. Under iron deficiency, MC-producing strains have a noted growth advantage over non-MC-producing strains and externally increase MC concentrations (Li *et al.*, 2009, Alexova *et al.*, 2011), and a recent study correlated MC production with chalkophore production (Li *et al.*, 2023), lending some evidence to a proposed role where cyanopeptides mediate metal homeostasis possibly by acting as a metal scavenger externally and as an absorbent intracellularly. MC null mutants in *Microcystis* have less resilience against oxidative stress (Zilliges *et al.*, 2011), and a majority of MCs are found intracellularly bound to microcystin-dependent proteins, many of which have been identified as redox-sensitive proteins from the Calvin-Benson-Bassham cycle (Malanga *et al.*, 2019). Cyanobacteria may produce cyanopeptides as a mechanism to protect themselves against reactive oxygen species generated by photosynthetic machinery, thereby limiting turnover of damaged proteins at the height of a cyanobacterial bloom when nutrients become scarce (Pineda-Mendoza *et al.*, 2016, Natumi & Janssen, 2020, Wagner *et al.*, 2021). Likewise, in growth limiting conditions, the *M. album* BG8 Mpt may prevent the generation of – or damage by – reactive oxygen species from pMMO or other oxidoreductases. Lastly, MC inhibits the growth of other cyanobacteria, algae, and aquatic plants upon release during cell lysis (Singh *et al.*, 2001, Silva & Vasconcelos, 2010), thus Mpt-mediated interspecies interactions also cannot be discounted. One such allelopathic mechanism occurs by inducing the secretion of alkaline phosphatases from phytoplankton via cyanopeptides as a method of acquiring phosphate in phosphate-limiting conditions (Oh *et al.*, 2000, Bar-Yosef *et al.*, 2010, Raven, 2010). As for *M. album* BG8, potential targets of Mpt could range from transporters, enzymes involved in Mbn synthesis, and other homeostasis machinery in species competing for the same copper.

(5.3) An ancestral nutrient stress response links methane oxidizing bacteria to cyanobacteria

Analysis of the *M. album* BG8 Mpt-BGC via BiG-SCAPE combined with methanobactin phylogenetic and core peptide analysis revealed close evolutionary relatives in cyanobacteria, indicating a common nutrient starvation stress response. A shared ancestral stress response by *M. album* BG8 and cyanobacteria may be counterintuitive, but since photosynthetic activity generates oxygen, cyanobacteria are ideal metabolic partners with MOB to exchange carbon dioxide for oxygen (Cerbin *et al.*, 2022), and methanogenesis can be promoted especially after a cyanobacterial bloom (Yu *et al.*, 2023) providing ample substrate for MOB. Cyanobacteria also require copper; electron transfer between cytochrome f to photosystem I relies on two metalloproteins with alternating cofactor redox states: the dominant, constitutively expressed copper-based plastocyanin or the iron-based cytochrome c_6 used during copper deficiency. A recent discovery found that cyanobacteria have their own “copper switch” based on a transcriptional regulator that represses plastocyanin expression in favor of cytochrome c_6 , and a protease flips this gene expression by degrading the regulator when copper is present (García-Cañas *et al.*, 2021). A strong correlation was also recently observed between chalkophore and MC production in *Microcystis* (Li *et al.*, 2021) underscoring MC as a putative alleviator of stress resulting from copper deficiency. Understanding how a common nutrient stress response was recruited to meet the needs of cohabitating bacteria with drastically contrasting metabolic lifestyles can further our insight into the purpose of biosynthetic gene cluster products in both MOB and cyanobacteria.

Similarity in both BGC sequences and their predicted products ties nutrient stress to secondary metabolites produced by symbionts. Patellamides produced by *Prochloron didemni* have long been hypothesized as the facilitator of its endosymbiosis with its host ascidian *Lissoclinum patella* (Baur *et al.*, 2022). However, how this occurs remains a mystery. *Prochloron* produces patellamides to maintain the concentration of copper 10^4 times higher than surrounding water within the host cloacal cavity where it resides. Yet, neither *Prochloron* nor its host *Lissoclinum* appear to require prodigious amounts of copper for their enzymology. Recent experiments demonstrated that copper(II)-bounded patellamides have efficient carbonic anhydrase activity like that of conventional zinc(II)-based carbonic anhydrases (Comba *et al.*, 2014). If nutrient deficiency – the underlying basis for Mbn and Mpt expression in *M. album* BG8 – similarly apply, perhaps patellamides alleviate nutrient stress by increasing carbon bioavailability in the host cloacal cavity by catalyzing carbon dioxide into soluble carbonic acid, allowing *Prochloron* to sufficiently

supply products of photosynthesis to *Lissoclinum*, thus enabling their endosymbiotic partnership over non-patellamide-producing candidates.

Likewise, examining the function of related cyanobacterial NPs can aid in elucidating the function of MOB BGCs. A recent study into an unrelated silent RiPP BGC centered on a cyanobacterial proteusin homolog to the gamma-MOB *Methylovulum psychotolerans* using heterologous expression of novel chimeric RiPPs and activity analysis (Nguyen *et al.*, 2022). While the function of these silent RiPP BGCs ultimately remained a mystery, future experiments to trigger the expression of silent BGCs can elucidate their functions in both cyanobacteria and MOB. However, functional analysis of novel BGCs remains a convoluted, piecemeal process necessitating the eventual integration of biology-driven omics-level data. Recent steps have been taken to enable BGC annotations from AI-based DeepBGC and GECCO software with 'rules-based' antiSMASH as the default base prediction engine, but harmonization between these platforms remains incomplete. The major limitation is generating antiSMASH outputs from the results generated from AI-based programs such as DeepBGC. Regardless of annotations supplemented from other platforms, antiSMASH only produces output files if it identifies gene clusters as a BGC. Thus, tools that rely on antiSMASH outputs would not be able to perform analyses on novel BGCs, as was the case with BiG-SCAPE and the RiPP BGC identified via DeepBGC in *M. album* BG8. Likewise for RiPPER, the RODEO module only recognized a single ABC type transporter gene as significant evidence for a BGC. Combined with the lack of curated homologs, established methodologies must be altered as subsequent automated programs fail to launch and phylogenetic analyses must be conducted separately. Inferring function also depends on searching a myriad collection of databases, some via analysis tools with their own internal databases (i.e. RiPPMiner, antiSMASH), to those specifically cataloguing by class or function of NPs (i.e. antimicrobials, NRPs), to pan BGC/NP collections like MIBiG and NPAtlas, each with varying methodologies and metrics for comparison from sequence similarity to predicted structure similarity. These comparisons necessitate a lower search score threshold depending on the novelty of the query. Ultimately, transcriptomics data from *M. album* BG8 has clarified predictions derived from a patchwork of software and databases and enabled a unifying interpretation of BGC function through identifying false negative results, precisely defining the borders of BGCs, and providing biological context for their expression.

(6) Conclusion

Examining the *M. albus* BG8 copper starvation response shines a spotlight on how BGCs and their NPs play a role in alleviating copper deficiency in MOB. While the discovery of novel, putative Mbn and Mpt BGCs still necessitates experimental confirmation of their product function, they highlight the redundant nature of copper acquisition in the pMMO-obligate *M. albus* BG8 by complementing a repertoire of copper acquisition mechanisms (Figure 6). In summary, *M. albus* BG8 can acquire copper via transporters, hoard them using CorA proteins, steal foreign Mbn, and produce its own Mbn when all else is insufficient.

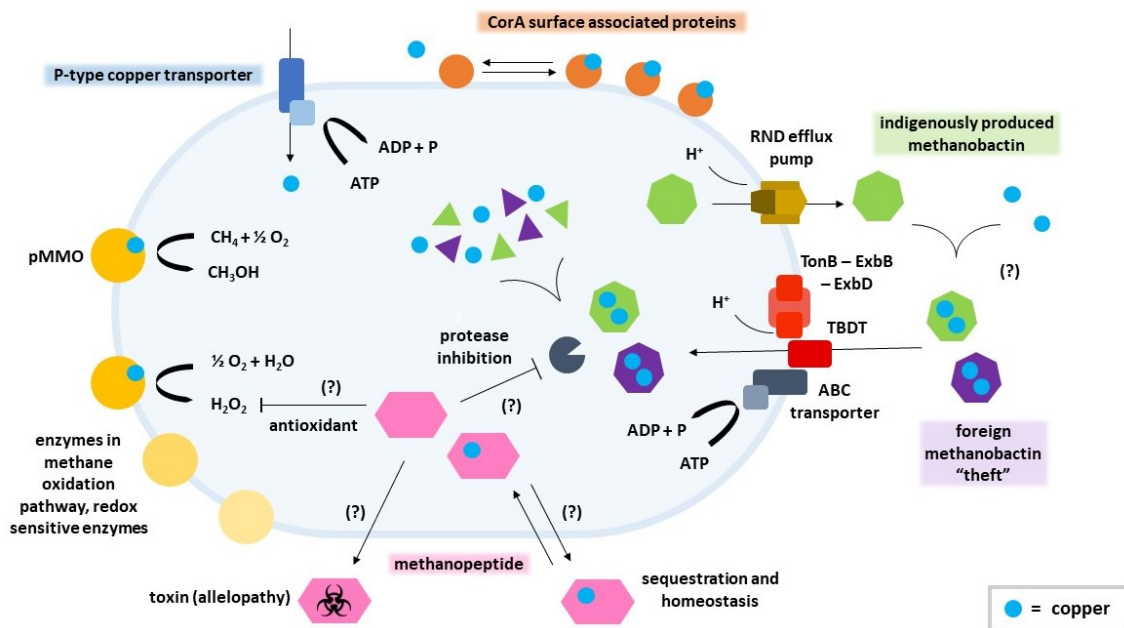


Figure 6. Summary figure of copper acquisition mechanisms of *M. albus* BG8. Question marks (?) indicate proposed processes based on gene expression and known functions of cyanobacterial NPs.

Otherwise, the result of severe copper starvation is the shuttering of most metabolism, an adverse outcome that intuitively would not bode well for survival and is best avoided. Yet dual variant MMO MOB avoid this adversity by maintaining their metabolism by switching to the iron-based sMMO. Presuming an incentive exists to avoid wholly shutting down its metabolism, are the redundant copper-competing strategies employed by pMMO-obligate MOB such as *M. albus* BG8 sufficient to compete against dual variant MMO

MOB in a copper limited environment? Can *M. album* BG8 retain a sufficient fraction of a limited supply of copper in polyculture over an extended period, assuming all other nutrients are supplied in excess and the eventual switching to sMMO by its competing MOB? Does copper speciation affect this competition? *Methylocystaceae* Mbn has a lower binding affinity to Cu (II), but rapidly reduces Cu(II) to Cu(I) upon binding (Choi *et al.*, 2006). Early characterizations of *M. album* BG8 Mbn suggested copper oxidation to be predominantly Cu(I) (Choi *et al.*, 2010), yet predicted models of *M. album* BG8 Mbn structure show similarity to Cu(II)-binding patellamide. Aside from the BGCs identified during copper starvation stress necessitating further research into the activity of their NPs, several predicted BGCs in *M. album* BG8 remain unexamined. What other stresses are specific secondary metabolites for in *M. album* BG8? How might these NPs allow *M. album* BG8 to alleviate stress? How well can biological context of distantly related NPs be used to inform research on stress responses of MOB and vice versa? Examining copper competitiveness along with other stress responses in MOB may yield insights into how different methanotrophs – nature’s sole biological methane sink – can thrive in environments prone to flux and disruption in a world undergoing rapid climate change.

(7) References

- Acharya D, Miller I, Cui YS, *et al.* (2019) Omics Technologies to Understand Activation of a Biosynthetic Gene Cluster in *Micromonospora* sp. WMMB235: Deciphering Keyicin Biosynthesis. *Acs Chemical Biology* **14**: 1260-1270.
- Agrawal P, Khater S, Gupta M, Sain N & Mohanty D (2017) RiPPMiner: a bioinformatics resource for deciphering chemical structures of RiPPs based on prediction of cleavage and cross-links. *Nucleic Acids Res* **45**: W80-w88.
- Akberdin IR, Collins DA, Hamilton R, Oshchepkov DY, Shukla AK, Nicora CD, Nakayasu ES, Adkins JN & Kaiyuzhnaya MG (2018) Rare Earth Elements Alter Redox Balance in *Methylobacterium alcaliphilum* 20Z(R). *Frontiers in Microbiology* **9**.
- Alexova R, Fujii M, Birch D, Cheng J, Waite TD, Ferrari BC & Neilan BA (2011) Iron uptake and toxin synthesis in the bloom-forming *Microcystis aeruginosa* under iron limitation. *Environmental Microbiology* **13**: 1064-1077.
- Amin SA, Moffett JW, Martens-Habbena W, Jacquot JE, Han Y, Devol A, Ingalls AE, Stahl DA & Armbrust EV (2013) Copper requirements of the ammonia-oxidizing archaeon *Nitrosopumilus maritimus* SCM1 and implications for nitrification in the marine environment. *Limnology and Oceanography* **58**: 2037-2045.
- Balado M, Osorio CR & Lemos ML (2006) A gene cluster involved in the biosynthesis of vanchrobactin, a chromosome-encoded siderophore produced by *Vibrio anguillarum*. *Microbiology-Sgm* **152**: 3517-3528.
- Balasubramanian R, Smith SM, Rawat S, Yatsunyk LA, Stemmler TL & Rosenzweig AC (2010) Oxidation of methane by a biological dicopper centre. *Nature* **465**: 115-U131.
- Bandow N, Gilles VS, Freesmeier B, *et al.* (2012) Spectral and copper binding properties of methanobactin from the facultative methanotroph *Methylocystis* strain SB2. *Journal of Inorganic Biochemistry* **110**: 72-82.
- Bar-Yosef Y, Sukenik A, Hadas O, Viner-Mozzini Y & Kaplan A (2010) Enslavement in the Water Body by Toxic *Aphanizomenon ovalisporum*, Inducing Alkaline Phosphatase in Phytoplanktons. *Current Biology* **20**: 1557-1561.
- Baur P, Kühl M, Comba P & Behrendt L (2022) Possible Functional Roles of Patellamides in the Ascidian-Prochloron Symbiosis. *Mar Drugs* **20**.
- Beck C, Gren T, Ortiz-Lopez FJ, *et al.* (2021) Activation and Identification of a Griseusin Cluster in *Streptomyces* sp. CA-256286 by Employing Transcriptional Regulators and Multi-Omics Methods. *Molecules* **26**.
- Behnsen J & Raffatellu M (2016) Siderophores: More than Stealing Iron. *Mbio* **7**.
- Berson O & Lidstrom ME (1996) Study of copper accumulation by the type I methanotroph *Methylobacterium albus* BG8. *Environmental Science & Technology* **30**: 802-809.
- Berson O & Lidstrom ME (1997) Cloning and characterization of *corA*, a gene encoding a copper-repressible polypeptide in the type I methanotroph, *Methylobacterium albus* BG8. *Fems Microbiology Letters* **148**: 169-174.

Bischoff K (2001) The toxicology of microcystin-LR: Occurrence, toxicokinetics, toxicodynamics, diagnosis and treatment. *Veterinary and Human Toxicology* **43**: 294-297.

Blin K, Shaw S, Kloosterman AM, Charlop-Powers Z, van Wezel GP, Medema MH & Weber T (2021) antiSMASH 6.0: improving cluster detection and comparison capabilities. *Nucleic Acids Research* **49**: W29-W35.

Brantner CA, Remsen CC, Owen HA, Buchholz LA & Collins MLP (2002) Intracellular localization of the particulate methane monooxygenase and methanol dehydrogenase in *Methylomicrobium album* BG8. *Archives of Microbiology* **178**: 59-64.

Brantner CA, Buchholz LA, McSwain CL, Newcomb LL, Remsen CC & Collins MLP (1997) Intracytoplasmic membrane formation in *Methylomicrobium album* BG8 is stimulated by copper in the growth medium. *Canadian Journal of Microbiology* **43**: 672-676.

Bratovanov EV, Ishida K, Heinze B, Pidot SJ, Stinear TP, Hegemann JD, Marahiel MA & Hertweck C (2020) Genome Mining and Heterologous Expression Reveal Two Distinct Families of Lasso Peptides Highly Conserved in Endofungal Bacteria. *ACS Chem Biol* **15**: 1169-1176.

Cao L, Do T & Link AJ (2021) Mechanisms of action of ribosomally synthesized and posttranslationally modified peptides (RiPPs). *Journal of Industrial Microbiology & Biotechnology* **48**.

Cao L, Gurevich A, Alexander KL, *et al.* (2019) MetaMiner: A Scalable Peptidogenomics Approach for Discovery of Ribosomal Peptide Natural Products with Blind Modifications from Microbial Communities. *Cell Systems* **9**: 600-+.

Carroll LM, Larralde M, Fleck JS, Ponnudurai R, Milanese A, Cappio E & Zeller G (2021) Accurate de novo identification of biosynthetic gene clusters with GECCO. *bioRxiv* 2021.2005.2003.442509.

Cerbin S, Perez G, Rybak M, *et al.* (2022) Methane-Derived Carbon as a Driver for Cyanobacterial Growth. *Frontiers in Microbiology* **13**.

Chang J, Gu WY, Park D, Semrau JD, DiSpirito AA & Yoon S (2018) Methanobactin from *Methylosinus trichosporium* OB3b inhibits N₂O reduction in denitrifiers. *ISME Journal* **12**: 2086-2089.

Chang J, Kim DD, Semrau JD, Lee JY, Heo H, Gu WY & Yoon S (2021) Enhancement of Nitrous Oxide Emissions in Soil Microbial Consortia via Copper Competition between Proteobacterial Methanotrophs and Denitrifiers. *Applied and Environmental Microbiology* **87**.

Chang WH, Lin HH, Tsai IK, Huang SH, Chung SC, Tu IP, Yu SSF & Chan SI (2021) Copper Centers in the Cryo-EM Structure of Particulate Methane Monooxygenase Reveal the Catalytic Machinery of Methane Oxidation. *Journal of the American Chemical Society* **143**: 9922-9932.

Chaston JM, Suen G, Tucker SL, *et al.* (2011) The entomopathogenic bacterial endosymbionts *Xenorhabdus* and *Photorhabdus*: convergent lifestyles from divergent genomes. *PLoS One* **6**: e27909.

Cheung-Lee WL & Link AJ (2019) Genome mining for lasso peptides: past, present, and future. *Journal of Industrial Microbiology & Biotechnology* **46**: 1371-1379.

Choi DW, Bandow NL, McEllistrem MT, *et al.* (2010) Spectral and thermodynamic properties of methanobactin from gamma-proteobacterial methane oxidizing bacteria: A case for copper competition on a molecular level. *Journal of Inorganic Biochemistry* **104**: 1240-1247.

Choi DW, Zea CJ, Do YS, *et al.* (2006) Spectral, Kinetic, and Thermodynamic Properties of Cu(I) and Cu(II) Binding by Methanobactin from *Methylosinus trichosporium* OB3b. *Biochemistry* **45**: 1442-1453.

Chowdhury TR & Dick RP (2013) Ecology of aerobic methanotrophs in controlling methane fluxes from wetlands. *Applied Soil Ecology* **65**: 8-22.

Christiansen G, Philmus B, Hemscheidt T & Kurmayer R (2011) Genetic Variation of Adenylation Domains of the Anabaenopeptin Synthesis Operon and Evolution of Substrate Promiscuity. *Journal of Bacteriology* **193**: 3822-3831.

Chu F & Lidstrom ME (2016) XoxF Acts as the Predominant Methanol Dehydrogenase in the Type I Methanotroph *Methylomicrobium buryatense*. *Journal of Bacteriology* **198**: 1317-1325.

Collins ML, Buchholz LA & Remsen CC (1991) Effect of Copper on *Methylomonas albus* BG8. *Applied and environmental microbiology* **57**: 1261-1264.

Comba P, Gahan LR, Hanson GR, Maeder M & Westphal M (2014) Carbonic anhydrase activity of dinuclear CuII complexes with patellamide model ligands. *Dalton Transactions* **43**: 3144-3152.

Cruz-Morales P, Kopp JF, Martinez-Guerrero C, Yanez-Guerra LA, Selem-Mojica N, Ramos-Aboites H, Feldmann J & Barona-Gomez F (2016) Phylogenomic Analysis of Natural Products Biosynthetic Gene Clusters Allows Discovery of Arseno-Organic Metabolites in Model Streptomyces. *Genome Biology and Evolution* **8**: 1906-1916.

Cusano AM, Burlinson P, Deveau A, Vion P, Uroz S, Preston GM & Frey-Klett P (2011) *Pseudomonas fluorescens* BBc6R8 type III secretion mutants no longer promote ectomycorrhizal symbiosis. *Environ Microbiol Rep* **3**: 203-210.

Dassa E & Bouige P (2001) The ABC of ABCs: a phylogenetic and functional classification of ABC systems in living organisms. *Research in Microbiology* **152**: 211-229.

Daumann LJ (2021) A Natural Lanthanide-Binding Protein Facilitates Separation and Recovery of Rare Earth Elements. *ACS Central Science* **7**: 1780-1782.

de Jong A, Kuipers OP & Kok J (2022) FUNAGE-Pro: comprehensive web server for gene set enrichment analysis of prokaryotes. *Nucleic Acids Research* **50**: W330-W336.

Deng YW, Ro SY & Rosenzweig AC (2018) Structure and function of the lanthanide-dependent methanol dehydrogenase XoxF from the methanotroph *Methylomicrobium buryatense* 5GB1C. *Journal of Biological Inorganic Chemistry* **23**: 1037-1047.

Diaz-Perez SP, Solis CS, Lopez-Bucio JS, Valdez Alarcon JJ, Villegas J, Reyes-De la Cruz H & Campos-Garcia J (2023) Pathogenesis in *Pseudomonas aeruginosa* PAO1 Biofilm-Associated Is Dependent on the Pyoverdine and Pyocyanin Siderophores by Quorum Sensing Modulation. *Microb Ecol* **86**: 727-741.

Dotson EM, Plikaytis B, Shinnick TM, Durvasula RV & Beard CB (2003) Transformation of *Rhodococcus rhodnii*, a symbiont of the Chagas disease vector *Rhodnius prolixus*, with integrative elements of the L1 mycobacteriophage. *Infect Genet Evol* **3**: 103-109.

Dou C, Long Z, Li S, *et al.* (2022) Crystal structure and catalytic mechanism of the MbnBC holoenzyme required for methanobactin biosynthesis. *Cell Research* **32**: 302-314.

Duan YW, Niu WJ, Pang LL, Bian XY, Zhang YM & Zhong GN (2022) Unusual Post-Translational Modifications in the Biosynthesis of Lasso Peptides. *International Journal of Molecular Sciences* **23**.

Dunfield PF, Yuryev A, Senin P, *et al.* (2007) Methane oxidation by an extremely acidophilic bacterium of the phylum Verrucomicrobia. *Nature* **450**: 879-U818.

Edgar RC & Soc IC (2004) MUSCLE: Multiple sequence alignment with improved accuracy and speed. *2004 IEEE Computational Systems Bioinformatics Conference, Proceedings* 728-729.

Egli CM, Natumi RS, Jones MR & Janssen EML (2020) Inhibition of Extracellular Enzymes Exposed to Cyanopeptides. *Chimia* **74**: 122-128.

Elsayed SS, Trusch F, Deng H, *et al.* (2015) Chaxapeptin, a Lasso Peptide from Extremotolerant *Streptomyces leeuwenhoekii* Strain C58 from the Hyperarid Atacama Desert. *The Journal of Organic Chemistry* **80**: 10252-10260.

Ewels PA, Peltzer A, Fillinger S, Patel H, Alneberg J, Wilm A, Garcia MU, Di Tommaso P & Nahnsen S (2020) The nf-core framework for community-curated bioinformatics pipelines. *Nature Biotechnology* **38**: 276-278.

Farhan UI Haque M, Kalidass B, Vorobev A, Baral BS, DiSpirito AA & Semrau JD (2015) Methanobactin from *Methylocystis* sp Strain SB2 Affects Gene Expression and Methane Monooxygenase Activity in *Methylosinus trichosporium* OB3b. *Applied and Environmental Microbiology* **81**: 2466-2473.

Felnagle EA, Jackson EE, Chan YA, Podevels AM, Berti AD, McMahon MD & Thomas MG (2008) Nonribosomal peptide synthetases involved in the production of medically relevant natural products. *Mol Pharm* **5**: 191-211.

Fouque KJD, Moreno J, Hegemann JD, Zirah S, Rebuffat S & Fernandez-Lima F (2018) Metal ions induced secondary structure rearrangements: mechanically interlocked lasso vs. unthreaded branched-cyclic topoisomers. *Analyst* **143**: 2323-2333.

Fru EC, Gray ND, McCann C, Baptista JD, Christgen B, Talbot HM, El Ghazouani A, Dennison C & Graham DW (2011) Effects of copper mineralogy and methanobactin on cell growth and sMMO activity in *Methylosinus trichosporium* OB3b. *Biogeosciences* **8**: 2887-2894.

Garber AI, Neelson KH, Okamoto A, McAllister SM, Chan CRS, Barco RA & Merino N (2020) FeGenie: A Comprehensive Tool for the Identification of Iron Genes and Iron Gene Neighborhoods in Genome and Metagenome Assemblies. *Frontiers in Microbiology* **11**.

García-Cañas R, Giner-Lamia J, Florencio FJ & López-Maury L (2021) A protease-mediated mechanism regulates the cytochrome c(6)/plastocyanin switch in *Synechocystis* sp. PCC 6803. *Proc Natl Acad Sci U S A* **118**.

Gavriš E, Sit CS, Cao SG, *et al.* (2014) Lassomycin, a Ribosomally Synthesized Cyclic Peptide, Kills *Mycobacterium tuberculosis* by Targeting the ATP-Dependent Protease ClpC1P1P2. *Chemistry & Biology* **21**: 509-518.

Gerlt JA, Bouvier JT, Davidson DB, Imker HJ, Sadkhin B, Slater DR & Whalen KL (2015) Enzyme Function Initiative-Enzyme Similarity Tool (EFI-EST): A web tool for generating protein sequence similarity networks. *Biochimica Et Biophysica Acta-Proteins and Proteomics* **1854**: 1019-1037.

Gilchrist CLM, Booth TJ, van Wersch B, van Grieken L, Medema MH & Chooi Y-H (2021) cblaster: a remote search tool for rapid identification and visualization of homologous gene clusters. *Bioinformatics Advances* **1**.

Gorman-Lewis D, Martens-Habbena W & Stahl DA (2019) Cu(II) adsorption onto ammonia-oxidizing bacteria and archaea. *Geochimica Et Cosmochimica Acta* **255**: 127-143.

Groom JD, Ford SM, Pesesky MW & Lidstrom ME (2019) A Mutagenic Screen Identifies a TonB-Dependent Receptor Required for the Lanthanide Metal Switch in the Type I Methanotroph "Methylotheobacterium bursariae" 5GB1C. *Journal of Bacteriology* **201**.

Gu WY & Semrau JD (2017) Copper and cerium-regulated gene expression in Methylosinus trichosporium OB3b. *Applied Microbiology and Biotechnology* **101**: 8499-8516.

Gu WY, Farhan UI Haque M, Baral BS, Turpin EA, Bandow NL, Kremmer E, Flatley A, Zischka H, DiSpirito AA & Semrau JD (2016) A TonB-Dependent Transporter Is Responsible for Methanobactin Uptake by Methylosinus trichosporium OB3b. *Applied and Environmental Microbiology* **82**: 1917-1923.

Gurevich A, Mikheenko A, Shlemov A, Korobeynikov A, Mohimani H & Pevzner PA (2018) Increased diversity of peptidic natural products revealed by modification-tolerant database search of mass spectra. *Nature Microbiology* **3**: 319-327.

Gwak JH, Awala SI, Nguyen NL, *et al.* (2022) Sulfur and methane oxidation by a single microorganism. *Proceedings of the National Academy of Sciences of the United States of America* **119**.

Hakemian AS & Rosenzweig AC (2007) The biochemistry of methane oxidation. *Annual Review of Biochemistry* **76**: 223-241.

Hannigan GD, Prihoda D, Palicka A, *et al.* (2019) A deep learning genome-mining strategy for biosynthetic gene cluster prediction. *Nucleic Acids Research* **47**.

Hanson RS & Hanson TE (1996) Methanotrophic bacteria. *Microbiological Reviews* **60**: 439-+.

He ZF, Cai CY, Wang JQ, Xu XH, Zheng P, Jetten MSM & Hu BL (2016) A novel denitrifying methanotroph of the NC10 phylum and its microcolony. *Scientific Reports* **6**.

Henard CA, Wu C, Xiong W, Henard JM, Davidheiser-Kroll B, Orata FD & Guarnieri MT (2021) Ribulose-1,5-Bisphosphate Carboxylase/Oxygenase (RubisCO) Is Essential for Growth of the Methanotroph Methylococcus capsulatus Strain Bath. *Applied and Environmental Microbiology* **87**.

Herfindal L, Myhren L, Kleppe R, Krakstad C, Selheim F, Jokela J, Sivonen K & Doskeland SO (2011) Nostocyclopeptide-M1: A Potent, Nontoxic Inhibitor of the Hepatocyte Drug Transporters OATP1B3 and OATP1B1. *Molecular Pharmaceutics* **8**: 360-367.

Hermenau R, Mehl JL, Ishida K, Dose B, Pidot SJ, Stinear TP & Hertweck C (2019) Genomics-Driven Discovery of NO-Donating Diazeniumdiolate Siderophores in Diverse Plant-Associated Bacteria. *Angew Chem Int Ed Engl* **58**: 13024-13029.

Hibi Y, Asai K, Arafuka H, Hamajima M, Iwama T & Kawai K (2011) Molecular structure of La³⁺-induced methanol dehydrogenase-like protein in Methylobacterium radiotolerans. *Journal of Bioscience and Bioengineering* **111**: 547-549.

IPCC (2023) Global Carbon and Other Biogeochemical Cycles and Feedbacks. *Climate Change 2021 – The Physical Science Basis: Working Group I Contribution to the Sixth Assessment Report of the Intergovernmental Panel on Climate Change*, (Intergovernmental Panel on Climate C, ed.) p.^pp. 673-816. Cambridge University Press, Cambridge.

Ito H, Yoshimori K, Ishikawa M, Hori K & Kamachi T (2021) Switching Between Methanol Accumulation and Cell Growth by Expression Control of Methanol Dehydrogenase in Methylosinus trichosporium OB3b Mutant. *Frontiers in Microbiology* **12**.

Itou Y, Ishida K, Shin SJ & Murakami M (1999) Oscillapeptins A to F, serine protease inhibitors from the three strains of *Oscillatoria agardhii*. *Tetrahedron* **55**: 6871-6882.

Janssen EML (2019) Cyanobacterial peptides beyond microcystins - A review on co-occurrence, toxicity, and challenges for risk assessment. *Water Research* **151**: 488-499.

Johnson KA, Ve T, Larsen O, Pedersen RB, Lillehaug JR, Jensen HB, Helland R & Karlsen OA (2014) CorA Is a Copper Repressible Surface-Associated Copper(I)-Binding Protein Produced in *Methylomicrobium album* BG8. *Plos One* **9**.

Jokela J, Herfindal L, Wahlsten M, Permi P, Selheim F, Vasconcelos V, Doskeland SO & Sivonen K (2010) A Novel Cyanobacterial Nostocyclopeptide is a Potent Antitoxin against Microcystins. *Chembiochem* **11**: 1594-1599.

Jones MR, Pinto E, Torres MA, *et al.* (2021) CyanoMetDB, a comprehensive public database of secondary metabolites from cyanobacteria. *Water Research* **196**.

Kalidass B, Farhan UI Haque M, Baral BS, DiSpirito AA & Semraua JD (2015) Competition between Metals for Binding to Methanobactin Enables Expression of Soluble Methane Monooxygenase in the Presence of Copper. *Applied and Environmental Microbiology* **81**: 1024-1031.

Kalyuzhnaya MG, Yang S, Rozova ON, *et al.* (2013) Highly efficient methane biocatalysis revealed in a methanotrophic bacterium. *Nature Communications* **4**: 2785.

Kang-Yun CS, Liang XJ, Dershwitz P, *et al.* (2022) Evidence for methanobactin "Theft" and novel chalkophore production in methanotrophs: impact on methanotrophic-mediated methylmercury degradation. *Isme Journal* **16**: 211-220.

Karlsen OA, Berven FS, Stafford GP, Larsen O, Murrell JC, Jensen HB & Fjellbirkeland A (2003) The surface-associated and secreted MopE protein of *Methylococcus capsulatus* (Bath) responds to changes in the concentration of copper in the growth medium. *Applied and Environmental Microbiology* **69**: 2386-2388.

Katoh K & Standley DM (2013) MAFFT multiple sequence alignment software version 7: improvements in performance and usability. *Mol Biol Evol* **30**: 772-780.

Kenney GE & Rosenzweig AC (2013) Genome mining for methanobactins. *Bmc Biology* **11**.

Kenney GE, Sadek M & Rosenzweig AC (2016) Copper-responsive gene expression in the methanotroph *Methylosinus trichosporium* OB3b. *Metallomics* **8**: 931-940.

Khadem AF, Pol A, Jetten MSM & den Camp H (2010) Nitrogen fixation by the verrucomicrobial methanotroph '*Methylacidiphilum fumariolicum*' SolV. *Microbiology-Sgm* **156**: 1052-1059.

Kits KD, Campbell DJ, Rosana AR & Stein LY (2015) Diverse electron sources support denitrification under hypoxia in the obligate methanotroph *Methylomicrobium album* strain BG8. *Frontiers in Microbiology* **6**.

Kloosterman AM, Medema MH & van Wezel GP (2021) Omics-based strategies to discover novel classes of RiPP natural products. *Current Opinion in Biotechnology* **69**: 60-67.

Knapp CW, Fowle DA, Kulczycki E, Roberts JA & Graham DW (2007) Methane monooxygenase gene expression mediated by methanobactin in the presence of mineral copper sources. *Proceedings of the National Academy of Sciences of the United States of America* **104**: 12040-12045.

Knittel K & Boetius A (2009) Anaerobic oxidation of methane: progress with an unknown process. *Annu Rev Microbiol* **63**: 311-334.

Koh EI & Henderson JP (2015) Microbial Copper-binding Siderophores at the Host-Pathogen Interface. *Journal of Biological Chemistry* **290**: 18967-18974.

Krentz BD, Mulheron HJ, Semrau JD, *et al.* (2010) A Comparison of Methanobactins from *Methylosinus trichosporium* OB3b and *Methylocystis* Strain SB2 Predicts Methanobactins Are Synthesized from Diverse Peptide Precursors Modified To Create a Common Core for Binding and Reducing Copper Ions. *Biochemistry* **49**: 10117-10130.

Larsen O & Karlsen OA (2016) Transcriptomic profiling of *Methylococcus capsulatus* (Bath) during growth with two different methane monooxygenases. *Microbiologyopen* **5**: 254-267.

Lawton TJ, Ham J, Sun TL & Rosenzweig AC (2014) Structural conservation of the B subunit in the ammonia monooxygenase/particulate methane monooxygenase superfamily. *Proteins-Structure Function and Bioinformatics* **82**: 2263-2267.

Lee HJ, Kim SY, Kim PJ, Madsen EL & Jeon CO (2014) Methane emission and dynamics of methanotrophic and methanogenic communities in a flooded rice field ecosystem. *Fems Microbiology Ecology* **88**: 195-212.

Lee SW, Keeney DR, Lim DH, Dispirito AA & Semrau JD (2006) Mixed pollutant degradation by *Methylosinus trichosporium* OB3b expressing either soluble or particulate methane monooxygenase: Can the tortoise beat the hare? *Applied and Environmental Microbiology* **72**: 7503-7509.

Letunic I & Bork P (2016) Interactive tree of life (iTOL) v3: an online tool for the display and annotation of phylogenetic and other trees. *Nucleic Acids Research* **44**: W242-W245.

Li B, Zhang X, Wu G, Qin B, Tefsen B & Wells M (2023) Toxins from harmful algal blooms: How copper and iron render chalkophore a predictor of microcystin production. *Water Research* **244**: 120490.

Li B, Zhang X, Deng J, Cheng Y, Chen Z, Qin B, Tefsen B & Wells M (2021) A new perspective of copper-iron effects on bloom-forming algae in a highly impacted environment. *Water Research* **195**: 116889.

Li HL, Murphy T, Guo J, Parr T & Nalewajko C (2009) Iron-stimulated growth and microcystin production of *Microcystis novacekii* UAM 250. *Limnologia* **39**: 255-259.

Maia LB, Moura JJG & Moura I (2015) Molybdenum and tungsten-dependent formate dehydrogenases. *Journal of Biological Inorganic Chemistry* **20**: 287-309.

Maksimov MO & Link AJ (2013) Discovery and Characterization of an Isopeptidase That Linearizes Lasso Peptides. *Journal of the American Chemical Society* **135**: 12038-12047.

Maksimov MO, Koos JD, Zong CH, Lisko B & Link AJ (2015) Elucidating the Specificity Determinants of the AtxE2 Lasso Peptide Isopeptidase. *Journal of Biological Chemistry* **290**: 30806-30812.

Malanga G, Giannuzzi L & Hernando M (2019) The possible role of microcystin (D-Leu(1) MC-LR) as an antioxidant on *Microcystis aeruginosa* (Cyanophyceae). In vitro and in vivo evidence. *Comparative Biochemistry and Physiology C-Toxicology & Pharmacology* **225**.

Martins J & Vasconcelos V (2015) Cyanobactins from Cyanobacteria: Current Genetic and Chemical State of Knowledge. *Mar Drugs* **13**: 6910-6946.

Mather RV, Larsen TJ, Brock DA, Queller DC & Strassmann JE (2023) Paraburkholderia symbionts isolated from Dictyostelium discoideum induce bacterial carriage in other Dictyostelium species. *Proc Biol Sci* **290**: 20230977.

Matsuda K, Kuranaga T, Sano A, Ninomiya A, Takada K & Wakimoto T (2019) The Revised Structure of the Cyclic Octapeptide Surugamide A. *Chem Pharm Bull (Tokyo)* **67**: 476-480.

Matthijs S, Brandt N, Ongena M, Achouak W, Meyer JM & Budzikiewicz H (2016) Pyoverdine and histocorrugatin-mediated iron acquisition in Pseudomonas thivervalensis. *Biometals* **29**: 467-485.

Merwin NJ, Mousa WK, Dejong CA, Skinnider MA, Cannon MJ, Li HX, Dial K, Gunabalasingam M, Johnston C & Magarvey NA (2020) DeepRiPP integrates multiomics data to automate discovery of novel ribosomally synthesized natural products. *Proceedings of the National Academy of Sciences of the United States of America* **117**: 371-380.

Miyaji A, Nitta M & Baba T (2019) Influence of copper ions removal from membrane-bound form of particulate methane monooxygenase from Methylosinus trichosporium OB3b on its activity for methane hydroxylation. *Journal of Biotechnology* **306**.

Mohimani H, Gurevich A, Mikheenko A, Garg N, Nothias LF, Ninomiya A, Takada K, Dorrestein PC & Pevzner PA (2017) Dereplication of peptidic natural products through database search of mass spectra. *Nature Chemical Biology* **13**: 30-37.

Monib M, Abd-el-Malek Y, Hosny I & Fayed M (1979) Associative symbiosis of Azotobacter chroococcum and higher plants. *Zentralbl Bakteriell Naturwiss* **134**: 133-139.

Nakagawa T, Mitsui R, Tani A, Sasa K, Tashiro S, Iwama T, Hayakawa T & Kawai K (2012) A Catalytic Role of XoxF1 as La³⁺-Dependent Methanol Dehydrogenase in Methylobacterium extorquens Strain AM1. *Plos One* **7**.

Natumi R & Janssen EML (2020) Cyanopeptide Co-Production Dynamics beyond Microcystins and Effects of Growth Stages and Nutrient Availability. *Environmental Science & Technology* **54**: 6063-6072.

Navarro-Munoz JC, Selem-Mojica N, Mullaney MW, *et al.* (2020) A computational framework to explore large-scale biosynthetic diversity. *Nature Chemical Biology* **16**: 60+.

Nguyen NA, Cong Y, Hurrell RC, Arias N, Garg N, Puri AW, Schmidt EW & Agarwal V (2022) A Silent Biosynthetic Gene Cluster from a Methanotrophic Bacterium Potentiates Discovery of a Substrate Promiscuous Proteusin Cyclodehydratase. *ACS Chem Biol* **17**: 1577-1585.

Niehs SP, Dose B, Scherlach K, Pidot SJ, Stinear TP & Hertweck C (2019) Genome Mining Reveals Endopyrroles from a Nonribosomal Peptide Assembly Line Triggered in Fungal-Bacterial Symbiosis. *ACS Chem Biol* **14**: 1811-1818.

Nikolouli K & Mossialos D (2012) Bioactive compounds synthesized by non-ribosomal peptide synthetases and type-I polyketide synthases discovered through genome-mining and metagenomics. *Biotechnology Letters* **34**: 1393-1403.

Nishizawa A, Bin Arshad A, Nishizawa T, Asayama M, Fujii K, Nakano T, Harada K & Shirai M (2007) Cloning and characterization of a new hetero-gene cluster of nonribosomal peptide synthetase and polyketide synthase from the cyanobacterium Microcystis aeruginosa K-139. *Journal of General and Applied Microbiology* **53**: 17-27.

Niswati A, Murase J, Asakawa S & Kimura M (2004) Analysis of communities of ammonia oxidizers, methanotrophs, and methanogens associated with microcrustaceans in the floodwater of a rice field microcosm. *Soil Science and Plant Nutrition* **50**: 447-455.

Nyerges G & Stein LY (2009) Ammonia cometabolism and product inhibition vary considerably among species of methanotrophic bacteria. *Fems Microbiology Letters* **297**: 131-136.

Nyerges G, Han SK & Stein LY (2010) Effects of Ammonium and Nitrite on Growth and Competitive Fitness of Cultivated Methanotrophic Bacteria. *Applied and Environmental Microbiology* **76**: 5648-5651.

Oh HM, Lee SJ, Jang MH & Yoon BD (2000) Microcystin production by *Microcystis aeruginosa* in a phosphorus-limited chemostat. *Applied and Environmental Microbiology* **66**: 176-179.

Orata FD, Meier-Kolthoff JP, Sauvageau D & Stein LY (2018) Phylogenomic Analysis of the Gammaproteobacterial Methanotrophs (Order Methylococcales) Calls for the Reclassification of Members at the Genus and Species Levels. *Frontiers in Microbiology* **9**.

Palazzotto E & Weber T (2018) Omics and multi-omics approaches to study the biosynthesis of secondary metabolites in microorganisms. *Current Opinion in Microbiology* **45**: 109-116.

Peng P, Kang-Yun CS, Chang J, Gu WY, DiSpirito AA & Semrau JD (2022) Two TonB-Dependent Transporters in *Methylosinus trichosporium* OB3b Are Responsible for Uptake of Different Forms of Methanobactin and Are Involved in the Canonical "Copper Switch". *Applied and Environmental Microbiology* **88**.

Pineda-Mendoza RM, Zuniga G & Martinez-Jeronimo F (2016) Microcystin production in *Microcystis aeruginosa*: effect of type of strain, environmental factors, nutrient concentrations, and N:P ratio on *mcyA* gene expression. *Aquatic Ecology* **50**: 103-119.

Piscon BaPEEaFBaSGaELaASaHAaRGaZRaG-MO (2023) The Effect of Outer Space and Other Environmental Cues on Bacterial Conjugation. *Microbiology Spectrum* **11**.

Pishchany G & Kolter R (2020) On the possible ecological roles of antimicrobials. *Molecular Microbiology* **113**: 580-587.

Pol A, Barends TRM, Dietl A, Khadem AF, Eygensteyn J, Jetten MSM & Op den Camp HJM (2014) Rare earth metals are essential for methanotrophic life in volcanic mudpots. *Environmental Microbiology* **16**: 255-264.

Qin W, Amin SA, Lundeen RA, *et al.* (2018) Stress response of a marine ammonia-oxidizing archaeon informs physiological status of environmental populations. *Isme Journal* **12**: 508-519.

Qiu QF, Conrad R & Lu YH (2009) Environmental, genomic and taxonomic perspectives on methanotrophic Verrucomicrobia. *Environmental Microbiology Reports* **1**: 355-361.

Raven JA (2010) Cyanotoxins: A Poison that Frees Phosphate. *Current Biology* **20**: R850-R852.

Rawlings ND, Alan J, Thomas PD, Huang XD, Bateman A & Finn RD (2018) The MEROPS database of proteolytic enzymes, their substrates and inhibitors in 2017 and a comparison with peptidases in the PANTHER database. *Nucleic Acids Research* **46**: D624-D632.

Rodriguez V (2022) Insights into post-translational modification enzymes from RiPPs: A toolkit for applications in peptide synthesis. *Biotechnology Advances* **56**.

- Russell AH & Truman AW (2020) Genome mining strategies for ribosomally synthesised and post-translationally modified peptides. *Computational and Structural Biotechnology Journal* **18**: 1838-1851.
- Saha R, Saha N, Donofrio RS & Bestervelt LL (2013) Microbial siderophores: a mini review. *Journal of Basic Microbiology* **53**: 303-317.
- Saha S, Esposito G, Urajova P, *et al.* (2020) Discovery of Unusual Cyanobacterial Tryptophan-Containing Anabaenopeptins by MS/MS-Based Molecular Networking. *Molecules* **25**.
- Santos-Aberturas J, Chandra G, Frattaruolo L, Lacroet R, Pham TH, Vior NM, Eyles TH & Truman AW (2019) Uncovering the unexplored diversity of thioamidated ribosomal peptides in Actinobacteria using the RiPPER genome mining tool. *Nucleic Acids Research* **47**: 4624-4637.
- Schmidt EW, Nelson JT, Rasko DA, Sudek S, Eisen JA, Haygood MG & Ravel J (2005) Patellamide A and C biosynthesis by a microcin-like pathway in *Prochloron didemni*, the cyanobacterial symbiont of *Lissoclinum patella*. *Proc Natl Acad Sci U S A* **102**: 7315-7320.
- Selem-Mojica N, Aguilar C, Gutierrez-Garcia K, Martinez-Guerrero CE & Barona-Gomez F (2019) EvoMining reveals the origin and fate of natural product biosynthetic enzymes. *Microbial Genomics* **5**.
- Semrau JD, DiSpirito AA, Gu WY & Yoon S (2018) Metals and Methanotrophy. *Applied and Environmental Microbiology* **84**.
- Semrau JD, DiSpirito AA, Obulisamy PK & Kang-Yun CS (2020) Methanobactin from methanotrophs: genetics, structure, function and potential applications. *Fems Microbiology Letters* **367**.
- Semrau JD, Jagadevan S, DiSpirito AA, *et al.* (2013) Methanobactin and MmoD work in concert to act as the 'copper-switch' in methanotrophs. *Environmental Microbiology* **15**: 3077-3086.
- Sharp CE, Smirnova AV, Graham JM, Stott MB, Khadka R, Moore TR, Grasby SE, Strack M & Dunfield PF (2014) Distribution and diversity of Verrucomicrobia methanotrophs in geothermal and acidic environments. *Environmental Microbiology* **16**: 1867-1878.
- Silva P & Vasconcelos V (2010) Allelopathic effect of *Cylindrospermopsis raciborskii* extracts on the germination and growth of several plant species. *Chemistry and Ecology* **26**: 263-271.
- Singh DP, Tyagi MB, Kumar A & Thakur JK (2001) Antialgal activity of a hepatotoxin-producing cyanobacterium, *Microcystis aeruginosa*. *World Journal of Microbiology & Biotechnology* **17**: 15-22.
- Sivonen K, Leikoski N, Fewer DP & Jokela J (2010) Cyanobactins-ribosomal cyclic peptides produced by cyanobacteria. *Appl Microbiol Biotechnol* **86**: 1213-1225.
- Stamatakis A (2014) RAxML version 8: a tool for phylogenetic analysis and post-analysis of large phylogenies. *Bioinformatics* **30**: 1312-1313.
- Steinle L, Maltby J, Treude T, Kock A, Bange HW, Engbersen N, Zopfi J, Lehmann MF & Niemann H (2017) Effects of low oxygen concentrations on aerobic methane oxidation in seasonally hypoxic coastal waters. *Biogeosciences* **14**: 1631-1645.
- Su G, Zopfi J, Niemann H & Lehmann MF (2022) Multiple Groups of Methanotrophic Bacteria Mediate Methane Oxidation in Anoxic Lake Sediments. *Frontiers in Microbiology* **13**.
- Sugden S, Lazic M, Sauvageau D & Stein LY (2021) Transcriptomic and Metabolomic Responses to Carbon and Nitrogen Sources in *Methylomicrobium album* BG8. *Applied and Environmental Microbiology* **87**.

Takeguchi M & Okura I (2000) Role of iron and copper in particulate methane monooxygenase of *Methylosinus trichosporium* OB3b. *Catalysis Surveys from Japan* **4**: 51-63.

Tavormina PL, Orphan VJ, Kalyuzhnaya MG, Jetten MSM & Klotz MG (2011) A novel family of functional operons encoding methane/ammonia monooxygenase-related proteins in gammaproteobacterial methanotrophs. *Environmental Microbiology Reports* **3**: 91-100.

Tays C, Guarnieri MT, Sauvageau D & Stein LY (2018) Combined Effects of Carbon and Nitrogen Source to Optimize Growth of Proteobacterial Methanotrophs. *Frontiers in Microbiology* **9**.

Tentori EF, Fang S & Richardson RE (2022) RNA Biomarker Trends across Type I and Type II Aerobic Methanotrophs in Response to Methane Oxidation Rates and Transcriptome Response to Short-Term Methane and Oxygen Limitation in *Methylomicrobium album* BG8. *Microbiology Spectrum* **10**.

Terlouw BR, Blin K, Navarro-Munoz JC, *et al.* (2023) MIBiG 3.0: a community-driven effort to annotate experimentally validated biosynthetic gene clusters. *Nucleic Acids Res* **51**: D603-D610.

Tietz JI, Schwalen CJ, Patel PS, Maxson T, Blair PM, Tai HC, Zakai UI & Mitchell DA (2017) A new genome-mining tool redefines the lasso peptide biosynthetic landscape. *Nature Chemical Biology* **13**: 470-+.

Um S, Kim Y-J, Kwon H, Wen H, Kim S-H, Kwon HC, Park S, Shin J & Oh D-C (2013) Sungsanpin, a Lasso Peptide from a Deep-Sea Streptomyces. *Journal of Natural Products* **76**: 873-879.

van den Brenk AL, Fairlie DP, Hanson GR, Gahan LR, Hawkins CJ & Jones A (1994) Binding of Copper(II) to the Cyclic Octapeptide Patellamide D. *Inorganic Chemistry* **33**: 2280-2289.

van Santen JA, Poynton EF, Iskakova D, *et al.* (2021) The Natural Products Atlas 2.0: a database of microbially-derived natural products. *Nucleic Acids Research* **50**: D1317-D1323.

Villada JC, Duran MF, Lim CK, Stein LY & Lee PKH (2022) Integrative Genome-Scale Metabolic Modeling Reveals Versatile Metabolic Strategies for Methane Utilization in *Methylomicrobium album* BG8. *Msystems* **7**.

Vorobev AV, Baani M, Doronina NV, Brady AL, Liesack W, Dunfield PF & Dedysh SN (2011) *Methyloferula stellata* gen. nov., sp. nov., an acidophilic, obligately methanotrophic bacterium that possesses only a soluble methane monooxygenase. *International Journal of Systematic and Evolutionary Microbiology* **61**: 2456-2463.

Wagner ND, Quach E, Buscho S, *et al.* (2021) Nitrogen form, concentration, and micronutrient availability affect microcystin production in cyanobacterial blooms. *Harmful Algae* **103**.

Waterhouse AM, Procter JB, Martin DMA, Clamp M & Barton GJ (2009) Jalview Version 2—a multiple sequence alignment editor and analysis workbench. *Bioinformatics* **25**: 1189-1191.

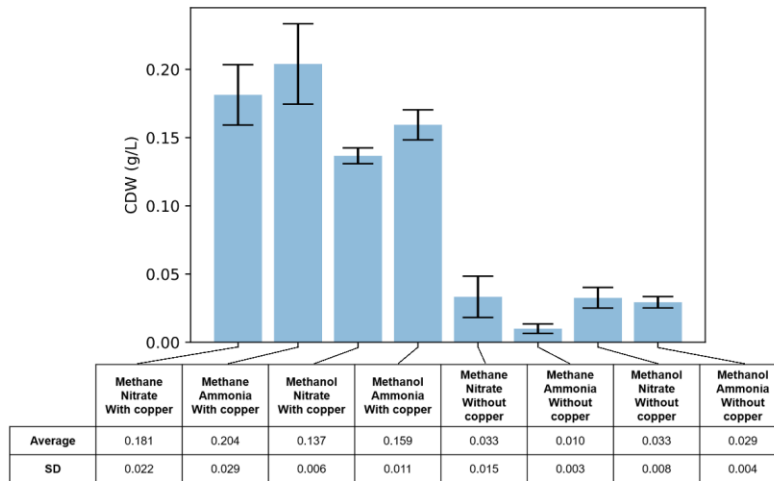
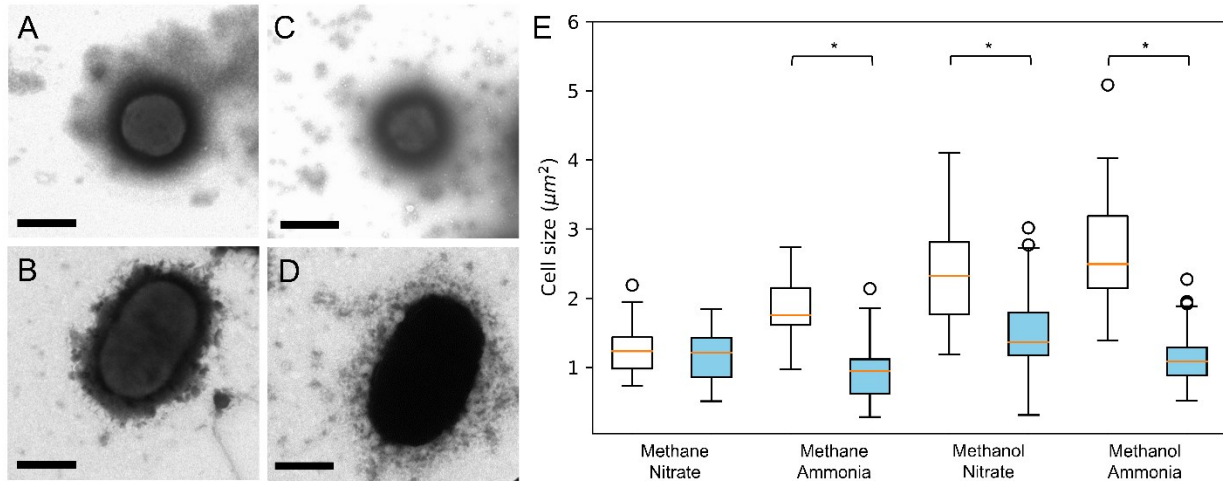
Welker M & von Dohren H (2006) Cyanobacterial peptides - Nature's own combinatorial biosynthesis. *Fems Microbiology Reviews* **30**: 530-563.

West CA, Salmond GPC, Dalton H & Murrell JC (1992) Functional expression in *Escherichia coli* of proteins B and C from soluble methane monooxygenase of *Methylococcus capsulatus* (Bath). *Microbiology* **138**: 1301-1307.

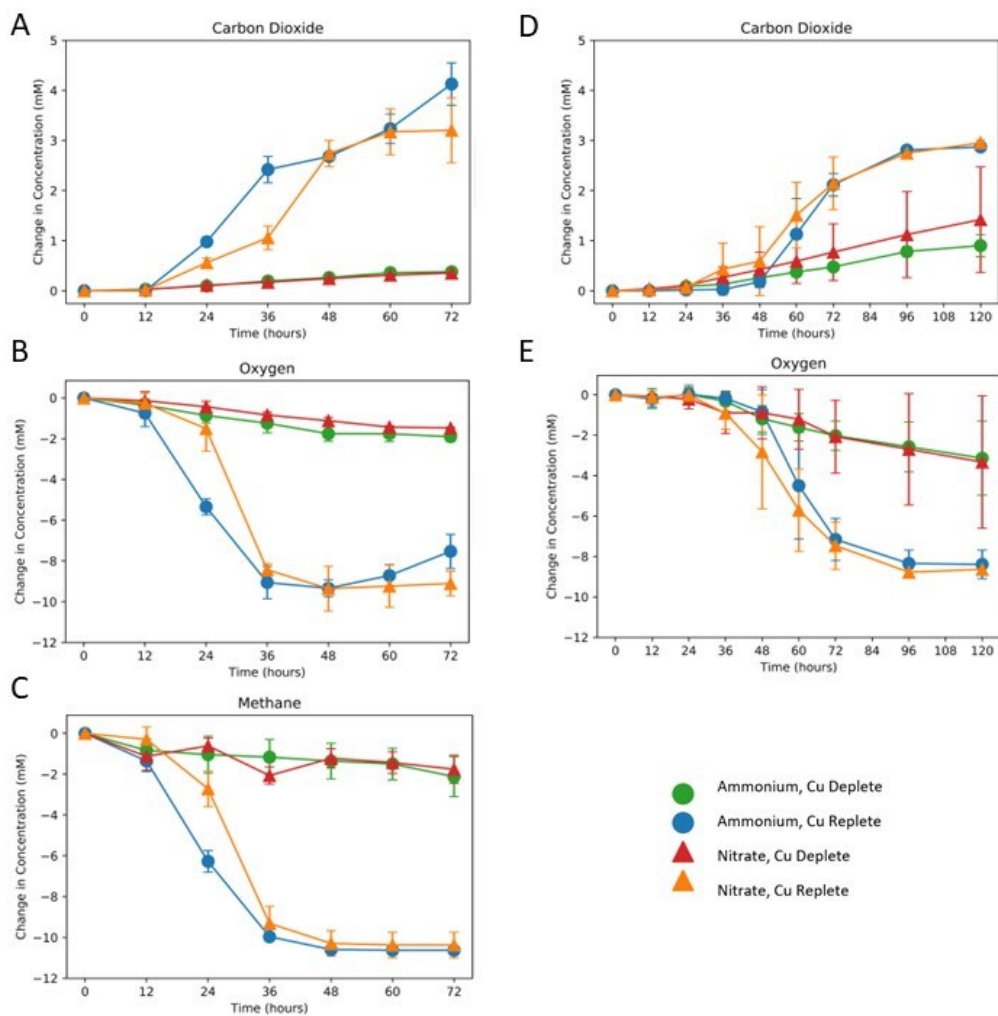
Wheeler JD, Secchi E, Rusconi R & Stocker R (2019) Not Just Going with the Flow: The Effects of Fluid Flow on Bacteria and Plankton. *Annual Review of Cell and Developmental Biology* **35**: 213-237.

- Whittenbury R, Phillips KC & Wilkinson JF (1970) Enrichment, isolation and some properties of methane-utilizing bacteria. *J Gen Microbiol* **61**: 205-218.
- Yeats C, Rawlings ND & Bateman A (2004) The PepSY domain: a regulator of peptidase activity in the microbial environment? *Trends in Biochemical Sciences* **29**: 169-172.
- Yu YM, Ouyang YD & Yao W (2018) shinyCircos: an R/Shiny application for interactive creation of Circos plot. *Bioinformatics* **34**: 1229-1231.
- Yu Z & Chistoserdova L (2017) Communal Metabolism of Methane and the Rare Earth Element Switch. *Journal of Bacteriology* **199**.
- Yu Z, Peng X, Liu LM, Yang JR, Zhai XY, Xue YY, Mo YY & Yang J (2023) Microbial one-carbon and nitrogen metabolisms are beneficial to the reservoir recovery after cyanobacterial bloom. *Science of the Total Environment* **856**.
- Yuan H, Collins MLP & Antholine WE (1999) Type 2 Cu²⁺ in pMMO from *Methylomicrobium album* BG8. *Biophysical Journal* **76**: 2223-2229.
- Zheng Y, Huang J, Zhao F & Chistoserdova L (2018) Physiological Effect of XoxG(4) on Lanthanide-Dependent Methanotrophy. *Mbio* **9**.
- Zilliges Y, Kehr JC, Meissner S, Ishida K, Mikkat S, Hagemann M, Kaplan A, Borner T & Dittmann E (2011) The Cyanobacterial Hepatotoxin Microcystin Binds to Proteins and Increases the Fitness of *Microcystis* under Oxidative Stress Conditions. *Plos One* **6**.
- Zorz JK, Kozłowski JA, Stein LY, Strous M & Kleiner M (2018) Comparative Proteomics of Three Species of Ammonia-Oxidizing Bacteria. *Frontiers in Microbiology* **9**.

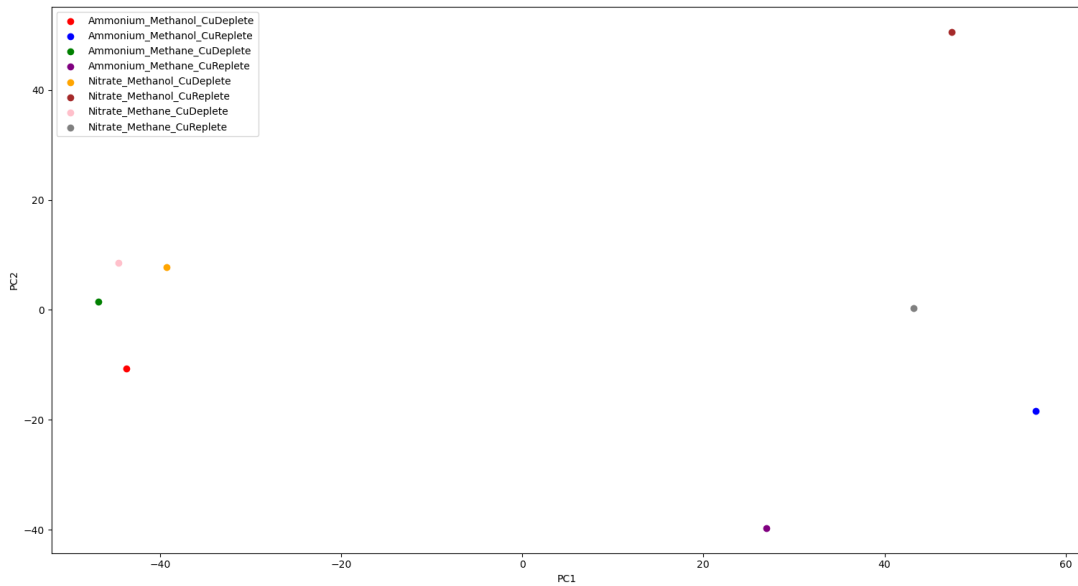
Appendix



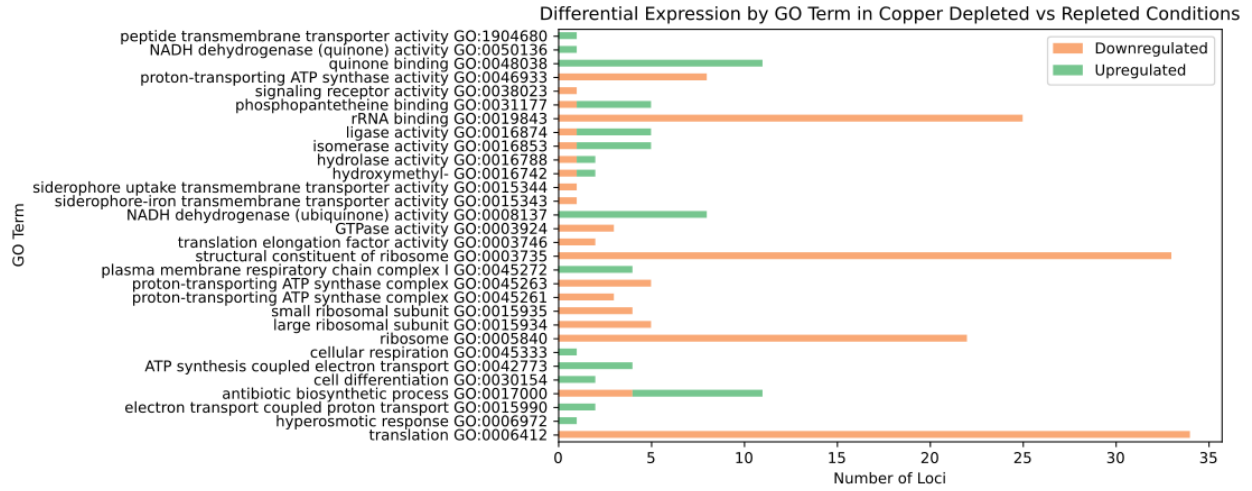
Appendix Figure 1. Physical characterization of *M. album* BG8. TEM cell images of *M. album* BG8 grown in 8 combinatorial nutrient conditions without copper in (A) methane and (C) methanol, and with copper in (B) methane and (D) methanol. (E) Sizes of cells ($n=50$) were plotted in white (copper replete) and blue (copper deplete) with the orange line representing the median. Significance from t tests ($p < 0.05$) are marked with an asterisk (*). (F) Cell dry weights are plotted in bar charts with confidence intervals plotted at 95%.



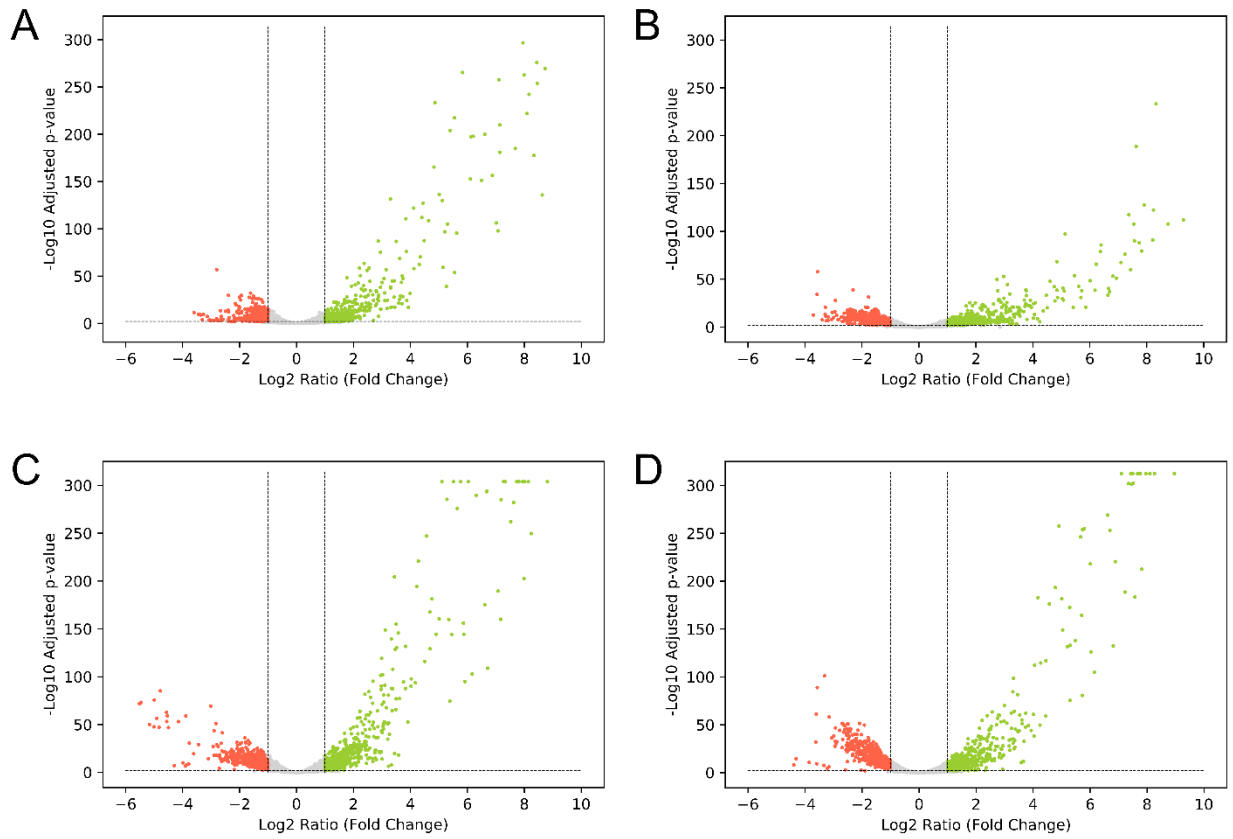
Appendix Figure 2. Change in concentration of gases measured from headspace of *M. album* BG8 cultures. (A, B, C) are grown in 2.5mmol methane, (D, E) are supplied with 2.5mmol methanol. Legend for nitrogen source and copper conditions located bottom right. Error bars indicate 95% confidence intervals.



Appendix Figure 3. PCA plots of transcriptome dataset. Averaged transcript counts across biological replicates from 8 combinatorial nutrient conditions. Percent variance scores for each principal component are PC1: 59.1%, PC2: 17.8% and PC3: 9.4%.



Appendix Figure 4. Gene set enrichment of genes in Gene Ontology terms. Stacked bar plot of number of gene loci upregulated and downregulated according to GO terms obtained from enrichment analysis via FUNAGE-Pro.



Appendix Figure 5. Volcano plots of differentially expressed genes. Copper depleted vs repleted conditions in (A) ammonium with methane, (B) ammonium with methanol, (C) nitrate with methane, and (D) nitrate with methanol (*adj. p* < 0.01, 2-fold change).

A

